Front. Chem. Sci. Eng. 2022, 16(1): 34–63
https://doi.org/10.1007/s11705-021-2050-1

REVIEW ARTICLE

Recent advances of small-molecule fluorescent probes for detecting biological hydrogen sulfide

Lei Zhou[1], Yu Chen[1], Baihao Shao[2], Juan Cheng[2], Xin Li (✉)[1,2]

1 Collaborative Innovation Center of Yangtze River Delta Region Green Pharmaceuticals, Zhejiang University of Technology, Hangzhou 310014, China
2 College of Pharmaceutical Sciences, Zhejiang University, Hangzhou 310058, China

© Higher Education Press 2021

Abstract H_2S is well-known as a colorless, acidic gas, with a notoriously rotten-egg smell. It was recently revealed that H_2S is also an endogenous signaling molecule that has important biological functions, however, most of its physiology and pathology remains elusive. Therefore, the enthusiasm for H_2S research remains. Fluorescence imaging technology is an important tool for H_2S biology research. The development of fluorescence imaging technology has realized the study of H_2S in subcellular organelles, facilitated by the development of fluorescent probes. The probes reviewed in this paper were categorized according to their chemical mechanism of sensing and were divided into three groups: H_2S reducibility-based probes, H_2S nucleophilicity-based probes, and metal sulfide precipitation-based probes. The structure of the probes, their sensing mechanism, and imaging results have been discussed in detail. Moreover, we also introduced some probes for hydrogen polysulfides.

Keywords hydrogen sulfide, fluorescent probe, reducibility, nucleophilicity, copper sulfide precipitate, hydrogen polysulfides

1 Introduction

H_2S has been demonstrated to act as a gas transmitter to exert functionally modulatory roles in human biology, similar to NO and CO. H_2S can render controllable regulation of cellular functions by affecting intracellular signaling processes. As an upstart among various vital biological gases, H_2S has received significant research interest, which has resulted in unraveling its biological functions in various cellular processes, especially in the cardiovascular system [1], inflammation system [2], nervous system [3].

One of the first observations of H_2S biology was its effect on the cardiovascular system. For instance, up-regulation of H_2S in rat blood vessels resulted in the expansion of vessels through opening of the vascular smooth muscle KATP channels [4]. In addition, in cecal ligation and puncture-induced rats, H_2S ameliorated cardiac dysfunction [5]. Up-regulation of cystathionine γ-lyase (CSE) *in vivo*, by means of increasing the local H_2S concentration, helped to protect experimental mice from the development of atherosclerosis [6]. In another study related to the evaluation of morpholin-4-ium-4-methoxyphenyl(mopholino) phosphinodithiote, a H_2S donor showed anti-atherosclerotic function [7].

Another most reported function of H_2S is its effect on the inflammatory system. In a recent study on H_2S, it was confirmed that levels of H_2S *in vivo* increased under inflammatory or sepsis conditions [2]. The interaction between H_2S and inflammatory attracts great attention. It was demonstrated that H_2S has a benign influence on mitigation of vascular inflammation via up-regulation of glutathione (GSH) and glutamate-cysteine (Cys) ligase catalytic subunit and inhibition of interleukin-1β in U937 monocytes [8]. It was demonstrated that exogenous H_2S can inhibit hyperplasia of the endothelial lining by partially restraining the interleukin-1β and selectively controlling mitogen-activated protein kinases and the phosphatidylinositol 3′-kinase/protein kinase B pathway on fibroblast-like synoviocytes, and can thus be used for the treatment of osteoarthritis [9].

The significant biological roles of H_2S have been revealed broadly and its importance obtains unprecedented attention. In addition to its effects on the cardiovascular system and inflammatory system, H_2S has also been closely related to Alzheimer's disease [10], Parkinson's

Received December 30, 2020; accepted February 15, 2021

E-mail: lixin81@zju.edu.cn

disease [11], gastrointestinal disease [12], and cancer [13]. Although there is still more to be studied, the functional roles of H_2S in human biology will be revealed clearly. Furthermore, depending on these developments, more effective and powerful H_2S-based therapeutic methods will be identified.

2 Current engineering strategies for detecting H_2S

H_2S *in vivo* is mainly derived from Cys and 3-mercaptopyruvate via enzymatic reactions catalyzed by cystathionine β-synthase (CBS), CSE, Cys aminotransferase, and 3-mercaptopyruvate sulfurtransferase [14]. However, due to the dynamic conversion between various H_2S-existing forms, the accurate biological concentration of H_2S *in vivo* is untraceable. For example, experiments conducted in the Whiteman lab revealed that the concentration of H_2S in healthy volunteers was around 43.8 ± 5 $\mu mol \cdot L^{-1}$, and was markedly increased (up to 200 $\mu mol \cdot L^{-1}$ in one case) during septic shock [15]. Therefore, reliable analytical assays that measure the accurate concentration of H_2S *in vivo* are warranted. In recent years, the technology of fluorescent sensing was employed and small-molecular fluorescent probes have been identified as promising tools to interrogate biological H_2S.

Effective fluorescence sensors for bio-imaging must conquer stringent requirements. First, the probe must be exclusively selective to its corresponding target substrate without being interfered by other co-existing substrates. Moreover, since most biochemical analytes are at low concentrations in their native environment, the sensitivity of the probe has to be ensured for low-abundant analytes. In addition, for further *in vivo* applications, the probe should do no harm to human biology and its reactive product ought to be non-toxic. Furthermore, optical properties, solubility, membrane permeability, etc. should be taken into consideration.

The relative high concentrations of other biological sulfur species, such as GSH and Cys residues, are among the most challenging factors for probes to selectively detect H_2S *in vivo* [16]. At present, based on the reductive and nucleophilic ability of H_2S and its high binding affinity towards Cu^{2+}, various reaction-based H_2S probes have been developed, and are generally categorized into three types: reduction-based H_2S probes, nucleophilicity-based probes, and copper sulfide (CuS)-based probes. Several review articles have comprehensively summarized these probes [17–20]. However, new probes have also been rapidly developed in the last few years. Furthermore, hydrogen polysulfides (H_2S_n) is the redox partner of H_2S in terms of chemical properties. They coexist in biological systems and collectively regulate the sulfur redox balance. To study the distribution and regulation mechanism of H_2S_n in organisms, a number of probes have been developed. In this minireview, a brief review of these probes will be summarized and they can be divided into four groups: H_2S reducibility-based probes, H_2S nucleophilicity-based probes, metal sulfide precipitation-based probes and H_2S_n probe. The detection performance of each probe and biological application are shown in Table 1.

3 Reducibility-based probes for H_2S

Since the 19th century, H_2S, sodium sulfide, and sodium hydrosulfide have been used as synthetic reducing agents. Utilizing the reducibility of H_2S, reduction-based probes, which are designed based on the nitrogen atom redox states, have been developed. Four categories of nitrogen-containing groups have been reported, including the azide group, the nitro group, the hydroxamino group as well as the azo group, thereby realizing pragmatic availability of reaction mechanisms and integrating diversity into reduction-based probes.

3.1 Probes based on reduction of azide group for sensing

Since the first successful attempt by the Chang group in 2011, the azide group has become the most widely used functionality to design reduction-based H_2S probes [21]. The detection occurs via the chemoselective reduction of azide to amine. To date, almost all fluorophores, including rhodamine and its derivatives, coumarin, 1,8-naphthalimide, have been utilized to carry the azide group to generate structurally diverse probes for H_2S [19]. As a H_2S reporter, the biocompatibility and the versatility of the azide group make it the most promising engineering strategy for sensing H_2S in human biology.

In 2016, Chen et al. reported probe 1 (DDP-1) that could distinguish H_2S and H_2S_n [22]. The probe utilized two specific groups for sensing H_2S and H_2S_n. H_2S_n are oxidative products of H_2S that have a weaker reducing ability; the azide group can differentiate H_2S from H_2S_n. Biological experiments also proved that probe 1 (DDP-1) has cell membrane permeability and can recognize H_2S and H_2S_n from a different emission spectrum in cells. In 2018, Zhao et al. generated fluorescent probe 2 (Flu-N_3) by removing the H_2S_n reactive site in probe 1 (DDP-1) [23]. Probe 2 (Flu-N_3) performed good sensitivity and selectivity for H_2S compared to other biothiols and triumphantly imaged H_2S *in vivo*. Moreover, Jiao et al. chose rhodamine B instead of fluorescein and introduced HClO-specific thiolactone to create a two-photon fluorescent probe 3 (RPC-1) [24]. Probe 3 (RPC-1) exhibits two emission bands corresponding to H_2S and HClO, respectively. Upon excitation with a two-photon laser, the presence of HClO/H_2S results in significant fluorescence enhancement within their own channels. Therefore, through simultaneously imaging H_2S and HClO, probe 3 (RPC-1) can evaluate drug-induced liver injury caused by antidepressants

Table 1 The detection performance of the fluorescent probes summarized in this minireview

Probe	Selectivity	Ex/Em/nm	Reported change in fluorescence	Limit of detection (LOD)	Biological system
H_2S reducibility-based probes					
1 (DDP-1)	H_2S/H_2S_n	360/452, 542		100 nmol·L^{-1} 24 nmol·L^{-1}	HeLa cells
2 (Flu-N_3)	H_2S	470/538	50-fold	0.031 μmol·L^{-1}	HepG-2 cells and nude mice
3 (RPC-1)	H_2S/HClO	360/445 545/580		192.1 nmol·L^{-1} 19.8 nmol·L^{-1}	HeLa cells, HepG-2 cells, RAW264.7 cells and drug-induced liver injury mice
4 (Lyso-HA-HS)	H_2S/HOCl	380/448 550/580	490-fold	3.4×10^{-7} mol·L^{-1} 7.3×10^{-8} mol·L^{-1}	HepG-2 cells and RAW264.7 cells
5 (Mito-HS)	H_2S	345/540	21-fold		HeLa cells and BALB/C nude mice with xenograft breast cancer tumor
6 (Lyso-HS)	H_2S	345/540	15-fold		HeLa cells and BALB/C nude mice with xenograft breast cancer tumor
7 (MT-HS)	H_2S	440/540	40-fold	1.65 μmol·L^{-1}	HeLa cells and fresh rat liver slices
8 (Na-H_2S-ER)	H_2S	440/545	45-fold	7.77×10^{-6} mol·L^{-1}	HeLa cells, living liver tissue slices and zebrafish
9 (ASNHN-N_3)	H_2S	454/545		0.75 μmol·L^{-1}	HeLa cells, RAW264.7 cells, the fresh liver tissues and heart arteries
10 (BN-H_2S)	H_2S	440/544		71 nmol·L^{-1}	HeLa cells and NIH 3T3 cells
11 (CouN_3-BC)	H_2S	405/450	35-fold		HeLa cells
12	H_2S	370/490		0.67 μmol·L^{-1}	HEK293A cells
13–14	H_2S				
15 (Mito-HS)	H_2S	380/450	~43-fold	24.3 nmol·L^{-1}	HeLa cells, MDA-MB-231 cells, DU145 cells and 3T3-L1 cells
16 (Lyso-C)	H_2S	355/458	> 20-fold	47 nmol·L^{-1}	HepG-2 cells
17 (1-H_2S)	H_2S	580/635	7-fold	~4.7×10^{-5} mol·L^{-1}	HeLa cells, zebrafish and fresh liver tissue slices of Kunming mice
18 (AC-N_3)	H_2S	360/500		18 nmol·L^{-1}	HeLa cells
19 (QME-N_3)	RSH/H_2S	350/–			MCF-7 cells
20 (TPC-N_3)	H_2S	–/498			HepG-2 cells and fresh liver and muscle slices of liver cirrhosis induction mice
21 (Lyso-HS)	H_2S	365/505	95-fold	214.5 nmol·L^{-1}	A549 cells, HepG-2 cells and rat renal tubular epithelial cells
22 (QL-Gal-N_3)	H_2S	365/521	102-fold	126 nmol·L^{-1}	HeLa, A549 cells and HepG-2 cells
23 (Gol-H_2S)	H_2S	405/515		0.11 μmol·L^{-1}	HeLa, EK293A cells and SMMC-7721 cells
24 (Diketopyrrolopyrrole, DPP-NO_2)	H_2S	506/550	800-fold	5.2 nmol·L^{-1}	HeLa cells
25	H_2S	485/522		2.55 μmol·L^{-1}	HepG-2 cells
26 (azo1)					
27 (azo2)	H_2S	468/517	103-fold	5 μmol·L^{-1}	Fresh male Sprague-Dawley (SD) rat blood plasma and tissues
28 (azo3)	H_2S	468/517	148-fold	500 nmol·L^{-1}	Fresh male SD rat blood plasma and tissues
29–32					
33 (PHS1)	H_2S	393/486		8.87 nmol·L^{-1}	HeLa cells
H_2S nucleophilicity-based probes					
34				190 nmol·L^{-1} (buffer) 380 nmol·L^{-1} (serum)	

(*Continued*)

Probe	Selectivity	Ex/Em/nm	Reported change in fluorescence	Limit of detection (LOD)	Biological system
35 (Cy-Cl)	H_2S	760/795			HeLa cells
36 (CyCl-1)	HS^-			0.16 μmol·L^{-1}	Living mice
37 (CyCl-2)	HS^-			0.37 μmol·L^{-1}	Living mice
38 (BH-HS)	H_2S	450/535	57-fold	1.7×10^{-6} mol·L^{-1}	HeLa cells
39 (CPC)	H_2S	410/474, 582	56-fold	40 nmol·L^{-1}	HeLa cells
40 (TP-PMVC)	H_2S	405/550		3.2 μmol·L^{-1}	A549 cells
41 (CP-H_2S)	H_2S	355/454, 573	252.7-fold	2.2×10^{-7} mol·L^{-1}	SMMC-7721 hepatoma cells
42 (Mi)	H_2S	520/596		15 nmol·L^{-1}	HeLa cells
43 (CyT)	H_2S	575/595, 655		7.33 nmol·L^{-1}	HeLa cells
44 (Indo-TPE-Indo)	H_2S	488/560, 710		0.19 μmol·L^{-1}	HeLa, MCF-7 and HUVEC cells
45 (TP-MIVC)	RNA/H_2S	488/625 405/550	12-fold	1.0×10^{-6} mol·L^{-1} 3.2×10^{-6} mol·L^{-1}	HeLa cells, zebrafish, normal mice and tumor mice
46 (CTN)	H_2S	370/424	200-fold	90 nmol·L^{-1}	HeLa cells
47 (Near-infrared (NIR)-HS)	H_2S	670/723	50-fold	38 nmol·L^{-1}	MCF-7 cells and living mice
48 (TPE-3)	H_2S	452/550		0.09 μmol·L^{-1}	HeLa cells, zebrafish
49 (TP-NIR-HS)	H_2S	800/675		83 nmol·L^{-1}	A375 cells and nude rat liver frozen slices
50 (2-CHO-OH)	H_2S	550/655	32-fold	8.3×10^{-8} mol·L^{-1}	HeLa cells
51 (NDCM-2)	H_2S	490/655	160-fold	58.797 nmol·L^{-1}	MCF-7 cells, the kidney tissue slices and living Kunming mice
52 (NIPY-DNP, 2,4-dinitro phenyl)	H_2S	340/505	273-fold	0.36 μmol·L^{-1}	A549 cells
53 (TMSDNPOB)	H_2S	574/592	30-fold	1.27 μmol·L^{-1}	HeLa cells and raw 264.7 macrophage cells
54 (LC-H_2S)	H_2S	571/664	27-fold	4.05 μmol·L^{-1}	HeLa cells
55 (A)	H_2S	440/537		49 nmol·L^{-1}	LoVo cells and SW480 cells
56 (DMC)	H_2S	384/547		0.069 μmol·L^{-1}	HeLa cells
57 (Cda-DNP)	H_2S	405/450	120-fold	0.18 μmol·L^{-1}	HeLa cells, A549 cells, HFL1 cells, and zebrafish
58 (NR-NO_2)	H_2S	675/710			L929 cells, HeLa cells, HCT-116 cells and BALB/c nude mice
59 (Mito-NIR-SH)	H_2S	670/720	14-fold	89.3 nmol·L^{-1}	HeLa cells
60 (DMOEPB)	H_2S				
61 (DMONPB)	H_2S	543/625		1.3 μmol·L^{-1}	RAW264.7 macrophages and HeLa cells and liver tissues of Kunming mice
62	H_2S	570/623			HCT-116 and CT-26 cells
63	H_2S	590/680	115-fold	11 nmol·L^{-1}	HCT16, HT29, A549, H1944, MCF-7, MDA-MB-468, MDA-MB-231, PANC1, HeLa, HepG-2 cells and Kunming living mice
64 (QCy7-HS)	H_2S	580/715	25-fold	1 μmol·L^{-1}	HeLa, HepG-2 cells and female BALB/c mice
65 (Z1)	H_2S	480/537		0.15 μmol·L^{-1}	Ec1 cells
66 (L)	H_2S	496/607		1.05×10^{-5} mol·L^{-1}	MCF-7 cells
67	H_2S, Cys/homo-cysteine (Hcy), GSH	415/465 415/465 415/465		0.10 μmol·L^{-1} 0.08 μmol·L^{-1} 0.06 μmol·L^{-1}	HeLa cells
68	H_2S	382/550			HeLa cells

(*Continued*)

Probe	Selectivity	Ex/Em/nm	Reported change in fluorescence	Limit of detection (LOD)	Biological system
69	H_2S	382/455		150 nmol·L^{-1}	HeLa cells
70	H_2S	502/530	65-fold	0.057 μmol·L^{-1}	HEK293A cells
71	H_2S	530/589	4.5-fold	0.58 μmol·L^{-1}	HEK293A cells
72	H_2S	565/585	19-fold	0.36 μmol·L^{-1}	HEK293A cells and zebrafish
73	H_2S	405/480	45-fold	9 μmol·L^{-1}	HEK293 cells and HeLa cells
74	H_2S	405/496	200-fold	0.9 μmol·L^{-1}	HEK293A cells, A549 cells and zebrafish
75	H_2S	394/486	45-fold	56 nmol·L^{-1}	HEK293 cells
76 (Endoplasmic reticulum (ER)-CN)	H_2S	383/490	6.5-fold	4.9 μmol·L^{-1}	HeLa cells
77	H_2S	395/532	68-fold	2.46 μmol·L^{-1}	HeLa cells
78	H_2S	346/516	25-fold	20 nmol·L^{-1}	A431 cells
79 (BDP-N1)	H_2S	540/587	150-fold	0.06 μmol·L^{-1}	A549 cells and zebrafish
80 (BDP-N2)	H_2S	625/587	170-fold	0.08 μmol·L^{-1}	A549 cells and zebrafish
81	H_2S/GSH Cys/Hcy	620/685 460/540	253-fold/448-fold	70 μmol·L^{-1}/0.38 μmol·L^{-1} 52 nmol·L^{-1}/38 nmol·L^{-1}	HeLa cells and living mice
82	H_2S	539/565	160-fold	4.80×10^{-8} mol·L^{-1}	HeLa cells
83 (NIR-H_2S)	H_2S	730/830	68-fold	2.7×10^{-7} mol·L^{-1}	MCF-7 cells, athymic nude mice and Kunming mice
84 (L)	H_2S	780/468	29-fold	24 nmol·L^{-1}	HeLa cells
85 (RHP)	H_2S	410/550, 475	4-fold		A549 cells
86 (RHP-2)	H_2S	415/467, 532	27-fold	270 nmol·L^{-1}	MCF-7 cells and mouse hippocampus
87	H_2S	465/520	80-fold	0.15 μmol·L^{-1}	HeLa cells
88 (NS1)	H_2S	365/539, 444		1.7×10^{-6} mol·L^{-1}	MCF-7 cells
89 (MeRho-TCA)	H_2S	476/520	65-fold		
90 (LR-H_2S)	H_2S	410/541, 475 (one-photon) 840/541,475 (two-photo)	80-fold	0.70 μmol·L^{-1}	SGC-7901 cells
91 (PyN_3)	H_2S	410/455		158 nmol·L^{-1}	MCF-7 cells, HeLa cells, zebrafish
92 (NIR-Az)	H_2S	680/720	200-fold	0.26 μmol·L^{-1}	HeLa cells, RAW 264.7 murine macrophages and BALB/c nude mice
93 (Mito-VS)	H_2S	370/510	7-fold	0.17 μmol·L^{-1}	HeLa cells
94 (BDP-N_3)	H_2S	475/515	10-fold	2.05 μmol·L^{-1}	HepG-2 cells
95 (Mito-N_3)	H_2S	680/736		20 nmol·L^{-1}	MCF-7 cells and BALB/c(nu/nu) mice
96	H_2S	485/610		5.7 nmol·L^{-1}	HeLa cells
97 (MF-N_3)	H_2S	530/560	16-fold	0.09 μmol·L^{-1}	HepG-2 cells
98 (HF-PBA)	H_2S/biothiols	345/520, 400		75 nmol·L^{-1}	HeLa cells
99 (HS-1)	H_2S	350/403, 519		0.020±0.001 mmol·L^{-1}	A549 cells
100 (DCM-PBA)	H_2S	560/680		1.1 nmol·L^{-1}	HeLa cells
101 (Cy-PBA)	H_2S	675/725		21 nmol·L^{-1}	A549 cells and nude mice
102	H_2S	380/495, 525		91 nmol·L^{-1}	HeLa cells
103	H_2S	560/633	25-fold	8.37 μmol·L^{-1}	Hi5 insect cells and *Caenorhabditis elegans*
104 (DCN-S)	H_2S	420/550, 580	5.7-fold	88 nmol·L^{-1}	HeLa cells
105 (HBTSeSe)	H_2S	380/460	47-fold	0.19 μmol·L^{-1}	RAW264.7 cells

(*Continued*)

Probe	Selectivity	Ex/Em/nm	Reported change in fluorescence	Limit of detection (LOD)	Biological system
106 (SFP-1)	H_2S	300/391			HeLa cells
107 (SFP-2)	H_2S	465/510	16-fold		HeLa cells
108 (ZS1)	H_2S	520/561	62-fold	2.5 μmol·L^{-1}	RAW 264.7 macrophage cells
109 (P1)	H_2S	378/524			HeLa cells
110 (P2)	H_2S	370/450			
111 (P3)	H_2S	375/500		50 nmol·L^{-1}	HeLa cells
112 (P5)	H_2S	485/638		0.9 μmol·L^{-1}	HeLa cells
113 (RB-PE-1)	H_2S	560/590			HeLa cells
114 (RB-PE-2)	H_2S	560/590			HeLa cells
115 (RB-PE-3)	H_2S	560/590			HeLa cells
116 (FEPO-1)	H_2S	455/522		14 μmol·L^{-1}	HeLa cells and zebrafish
117 (FLVN-OCN)	H_2S	415/525		0.25 μmol·L^{-1}	A-549 cells
118 (ZX-NIR)	H_2S	520/600 650/700		37 nmol·L^{-1}	HCT116 cells, HepG-2 tumor-bearing mouse model and HCT116 tumor-bearing mice
119 (Coumarin-tetrazine (Tz))	H_2S	375/456	16-fold		
120 (boradiazaindacene (BODIPY)-Tz-I)	H_2S	580/660	22.7-fold	0.68 μmol·L^{-1}	3T3 fibroblast cells
121 (BODIPY-Tz-II)	H_2S	580/660	31-fold	0.66 μmol·L^{-1}	3T3 fibroblast cells
122	H_2S			18.2 μmol·L^{-1}	
123 (PTZ-P1)	H_2S	–/488	25-fold		
124 (PTZ-P2)	H_2S				
125 (PTZ-P3)	H_2S	330/480, 540			
126 (PTZ-P4)	H_2S	580/638			HeLa cells and *Caenorhabditis elegans*
H_2S metal sulfide-based fluorescent probes					
127	H_2S	470/517		420 nmol·L^{-1}	
128	Cu^{2+}/H_2S	410/505		1.3×10^{-7} mol·L^{-1}	HeLa cells
129	H_2S	456/612		0.25 μmol·L^{-1}	
130 (CuHCD)	S^{2-} and HNO	484/595 484/595		0.7 μmol·L^{-1} 23 μmol·L^{-1}	
131 (TACN)	H_2S				
132 (Cyclam)	H_2S				
133 (Hsip-1)	H_2S	491/516	50-fold		HeLa cells
134 (TMCyclen)	H_2S				
135	H_2S	680/765		80 nmol·L^{-1}	RAW264.7 cells and HEK 293 cells
136	H_2S	600/680			MCF-7 cells
137	H_2S	446/605	~130-fold	21.6 nmol·L^{-1}	
138 [Cu(MaT-cyclen)$_2$]	H_2S	375/430		205 nmol·L^{-1}	HeLa cells and zebrafish
139	H_2S	–/794	27-fold	280 nmol·L^{-1}	
140 (L1Cu)	H_2S	495/534			HeLa cells and L929 mouse fibroblast cell lines
141 (L1)	H_2S	494/523	25-30-fold	1.7 μmol·L^{-1}	HepG-2 cells
142 (L_1-Cu)	H_2S	495/557			HeLa cells

(*Continued*)

Probe	Selectivity	Ex/Em/nm	Reported change in fluorescence	Limit of detection (LOD)	Biological system
143 (L_2)					
144 (L)	Cu^{2+}/H_2S	310/373,495		9.12×10^{-7} mol·L^{-1}	
145 (NJ1)	Cu^{2+}/H_2S	360/492			HeLa cells
146 (NL)	Cu^{2+}/H_2S	430/519		0.17 μmol·L^{-1}	MDA-MB-231 cells
147	Cu^{2+}/HS^-	340/480	25-fold	2.24 μmol·L^{-1}	HepG-2 cells
148	Cu^{2+}/H_2S	345/540			
149	Cu^{2+}/H_2S	405/540		47 nmol·L^{-1}	NIH/3T3 cells
150 (TAB-3)					
151 (CAH-Cu^{2+})	H_2S	350/425	31-fold	65 nmol·L^{-1}	
152 (L-Cu)	H_2S	495/525		31 nmol·L^{-1}	HeLa cells and zebrafish
153 (DPD-Cu^{2+})	Cu^{2+}/S^{2-}	440/510 440/510		0.73 nmol·L^{-1} 0.87 nmol·L^{-1}	A549 cells
154 (Cu-1)	HS^-	543/600	14-fold		HeLa cells
155 ($Cu(BB)_2$)	H_2S	384/590		0.11 μmol·L^{-1}	
156 (aggregation-induced emission (AIE)-S)	Cu^{2+}/H_2S	350/533			HeLa cells
157 (6-CdII)	H_2S	550/599, 619			HeLa cells
158	H_2S	365/500	~13-fold	30 nmol·L^{-1}	
Fluorescent probes for H_2S_n					
159 (Cy-S_n)	H_2S_n	680/720		2.2×10^{-8} mol·L^{-1}	RAW264.7 cells and living mice
160 (KB1)	H_2S_n	535/682	> 30-fold	8.2 nmol·L^{-1}	MCF-7 cells
161 (RPHS1)	H_2S_n	395/482, 655	5.8-fold	43 nmol·L^{-1}	HeLa cells
162	H_2S_n	397/534	328-fold	26 nmol·L^{-1}	A549 cells and zebrafish
163 (PZC-S_n)	H_2S_n	480/620		1 nmol·L^{-1}	RAW 264.7 cells and zebrafish
164 (Re-SS)	H_2S_n	550/589		24 nmol·L^{-1}	RAW 246.7 cells
165 (BDP-PHS)	H_2S_n	525/574, 618		57 nmol·L^{-1}	HeLa cells
166 (JCCF)	H_2S_n	480/543	52-fold	98.3 nmol·L^{-1}	MCF-7 cells and zebrafish
167	H_2S_n	360/502	18-fold	5.0×10^{-7} mol·L^{-1}	HepG-2 cells
168	H_2S_n H_2S	410/468, 606 410/519, 606	194-fold 37-fold	21 nmol·L^{-1} 34 nmol·L^{-1}	RAW264.7 cells, living mice liver tissue and zebrafish
169 (NIPY-NF)	H_2S_n	340/520	69-fold	84 nmol·L^{-1}	A549 cells
170 (Lyso-NRT-HP)	H_2S_n	405/548		10 nmol·L^{-1}	HeLa cells and the freezing kidney slices
171 (BCy-FN)	H_2S_n	653/727		46 nmol·L^{-1}	RAW264.7 cells, ZF4 cells, zebrafish larvae and BALB/c mice
172	H_2S_n	680/708	44-fold	35 nmol·L^{-1}	HeLa cells, RAW264.7 cells and BALB/c mice
173 (τ-Probe)	H_2S_n			2 nmol·L^{-1}	HeLa cells and zebrafish
174 (MB-S_n)	H_2S_n	530/584		26.01 nmol·L^{-1}	RAW 264.7 cells
175 (HQO-PSP)	H_2S_n	520/633	86-fold	95.2 nmol·L^{-1}	A549 cells and mouse lung tissues
176 (SPS-M1)	H_2S_n	372/430, 506		0.1 μmol·L^{-1}	HeLa cells, transgenic mice expressing human A53 T α-syn, SH-SY5Y cells and fresh mice brain slices
177 (PP-PS)	H_2S_n	300/478	20.3-fold	1 nmol·L^{-1}	A549 cells, mouse tumor tissues and inflamed mouse models

duloxetine and fluoxetine, and explore the molecular mechanism associated with H_2S protection. In 2019, another multi-responsive probe 4 (Lyso-HA-HS) was developed utilizing diformylhydrazine as the HOCl reaction site, which can simultaneously detect H_2S and HOCl in lysosomes [25]. This probe was the first to track endogenous H_2S and HOCl in lysosomes in living cells.

Fluorescent probes based on 1,8-naphthalimide have been widely utilized in detecting H_2S. However, the ineffectiveness of the organelle targeting ability has not been resolved. Wu et al. developed two fluorescence probes 5 (Mito-HS) and 6 (Lyso-HS) for sensing H_2S in mitochondria and lysosomes by introducing triphenylphosphonium and dimethylamino moieties for organelle targeting [26]. These two probes showed a better response to H_2S than structurally similar probes that are not charged. In addition, probe 5 (Mito-HS) was applied to image H_2S in tumors in living mice. Furthermore, to explain the complexity of physiological H_2S in subcellular organelles, Deng et al. developed two-photon fluorescent H_2S probe 7 (MT-HS) with mitochondrial-targeting ability, which can be utilized for imaging H_2S in deep penetrating living tissue [27]. Furthermore, they designed an ER-targeted fluorescent H_2S probe 8 (NaH_2S-ER) by using a sulfanilamide group as the target group [28]. Since none of probes can be used to monitor intercellular transmission of H_2S, Fu et al. developed H_2S probe 9 (ASNHN-N_3), which showed good specificity on the cell surface with a long hydrophobic alkyl chain [29]. As expected, probe 9 (ASNHN-N_3) visualized H_2S in the cell membrane of living cells. Moreover, since H_2S is closely related to tumor growth, it is of importance to monitor the H_2S level in real-time for understanding its effects in tumor diagnosis and cancer cell proliferation. Therefore, Lin's group developed a novel fluorescent probe 10 (BN-H_2S) with a biotin group for detecting H_2S, which has a special selectivity for cell cancer [30]. Because of the selectivity of the biotin group, probe 10 (BN-H_2S) is capable of sensing H_2S in cancer cells by two-photon imaging.

High quantum yield, as well as the small molecular and favorable permeability make coumarin a widely-applied fluorophore. Exploiting the protein labeling technologies, Chen et al. obtained a coumarin-based H_2S probe 11 (CouN_3BC), which connected a CLIP-tag substrate and had specifically targeting ability for the nucleus and mitochondria [31]. Utilizing coumarin as the fluorophore core, Zhu et al. modified the 4 and 6 positions of the coumarin ring and synthesized a series of multi-fluorinated fluorescent probes 12–14 to achieve a fast response for real-time H_2S detection [32]. The data showed that increasing fluorine-substitution accelerated the H_2S-mediated reduction reaction, and the tetra-fluorinated coumarin probe 14 showed a very fast response and outstanding selectivity to H_2S both *in vitro* and *in vivo*. In addition, there are coumarin-based organelle targeting probes, of which Velusamy et al. developed chemodosimeter "off-on" fluorescent probe 15 (Mito-HS) [33]. Probe 15 (Mito-HS) quickly detected the formation of endogenous H_2S in cancer cells with no external stimulations. Furthermore, specific fluorescence imaging in cancer cells showed that probe 15 (Mito-HS) can make a distinction between normal cells and cancer cells according to the level of H_2S formation *in vivo*. Moreover, a commercially available fluorescent H_2S probe was rendered to target lysosome (16) (Lyso-C) [34]. When it was employed in cell imaging studies, probe 16 (Lyso-C) can distinguish diverse levels of H_2S in live cells and sensitively respond to exogenous H_2S in lysosomes.

Other fluorophores were exploited to carry the azide group. In 2017, Liu et al. developed a biphoton fluorescent probe 17 (1-H_2S), which was constructed through expanding the conjugation system of naphthalene and a coumarin analogue [35]. In biological experiments, probe 17 (1-H_2S) was found to aggregate in the nucleolus region where H_2S can be detected. By introducing azide at the 6-position of the chroman dye, Qiao et al. obtained a fluorescent probe 18 (AC-N_3) [36]. Probe 18 (AC-N_3) exhibited a better selectivity without interference from analytes, high sensitivity, and little cytotoxicity. In addition, the quinoline skeleton was employed to construct H_2S probes. Based on the quinoline scaffold, Dai et al. prepared a two-input fluorescent probe 19 (QME-N_3) [37]. This probe could generate intensive fluorescence sense RSH via the Michael addition and independently detected H_2S through reduction of the azide group. In 2018, Ren et al. reasonable designed a novel series of electron donor-acceptor type green fluorescent protein fluorophore scaffolds, which will improve the two-photon efficiency after forming a hydrogen-bond net in water [38]. For its excellent properties, Ren et al. developed a H_2S selective probe 20 (TPC-N_3) based on new scaffolds. Probe 20 (TPC-N_3) had a good deep-tissue penetration for imaging H_2S in the liver tissue. Accordingly, utilizing the click reaction, Dou et al. obtained fluorescent probe 21 (Lyso-HS), which introduced a tertiary amine as a lysosome-targeted moiety [39]. Probe 21 (Lyso-HS) showed enhanced fluorescence by 95-fold after sensing H_2S and was applied to detect lysosomal H_2S in living cells. In addition, probes 22 (QL-Gal-N_3) and 23 (Gol-H_2S) were successfully employed for respectively sensing endogenous H_2S in hepatocyte and the Golgi apparatus by incorporating different organelle targeting groups [40,41]. Probe 22 (QL-Gal-N_3) was developed through the introduction of a glycosyl moiety (as a hepatocyte targeting agent) to a quinoline fluorophore. In the presence of a glycosyl moiety, the water solubility and hepatocyte-targeting ability were obviously enhanced. Notably, probe 22 (QL-Gal-N_3) was utilized to detect H_2S in water samples and hepatocytes. Furthermore, the Golgi apparatus also played a significant role in eukaryotic organelles,

which revealed a cytoprotective role of H_2S in various physiological activities. Furthermore, Zhu and Sheng et al. developed a simple Golgi targeting fluorescent probe 23 (Gol-H_2S) for accurate and sensitive detection of H_2S. Considering the high cholesterol content of the Golgi membrane, a trifluoromethyl moiety was introduced into the quinoline structure to improve its fat solubility. Thus, probe 23 (Gol-H_2S) could easily enter the Golgi apparatus through the barrier of the Golgi membrane because of its lipophilicity. Additionally, probe 23 (Gol-H_2S) could monitor basal H_2S and changes in the Golgi apparatus of cells and zebrafish. More importantly, real-time visualization of H_2S production in the stress-induced Golgi apparatus was achieved by probe 23 (Gol-H_2S). Chemical structures of azide-based probes are shown in Fig. 1.

Taken together, the azide group is an ideal H_2S trigger, and these probes have good compatibility with biological systems. Moreover, they are not difficult to synthesize. Attention must be paid to the use of sodium azide because of its explosive nature. The potential flaw of such probes is its photoactivation, after continuous exposure to an optical microscope [42].

3.2 Probes based on reduction of nitro group for sensing

In addition to the azide group, other functional groups can be reduced by H_2S. One is nitro, which can be reduced to an amino group by H_2S. In 2017, a nitroolefin functionalized probe 24 (DPP-NO_2) was generated by Wang's group [43]. Taking advantage of its easy synthesis and modification, light resistance, and solvent resistance performances, DPP was chosen as the fluorophore, which has a red and high-performance pigment. Probe 24 (DPP-NO_2) showed almost 800-fold enhanced fluorescence after the nitro reaction. Furthermore, probe 24 (DPP-NO_2) was successfully used for imaging the fluorescence toward H_2S in HeLa cells. In 2019, Zhou et al. developed a BODIPY-based probe 25 that introduced isoxazole to strengthen the oxidizability speed of the nitro group, and resulted in a significantly reduced response time within 55 s [44]. Due

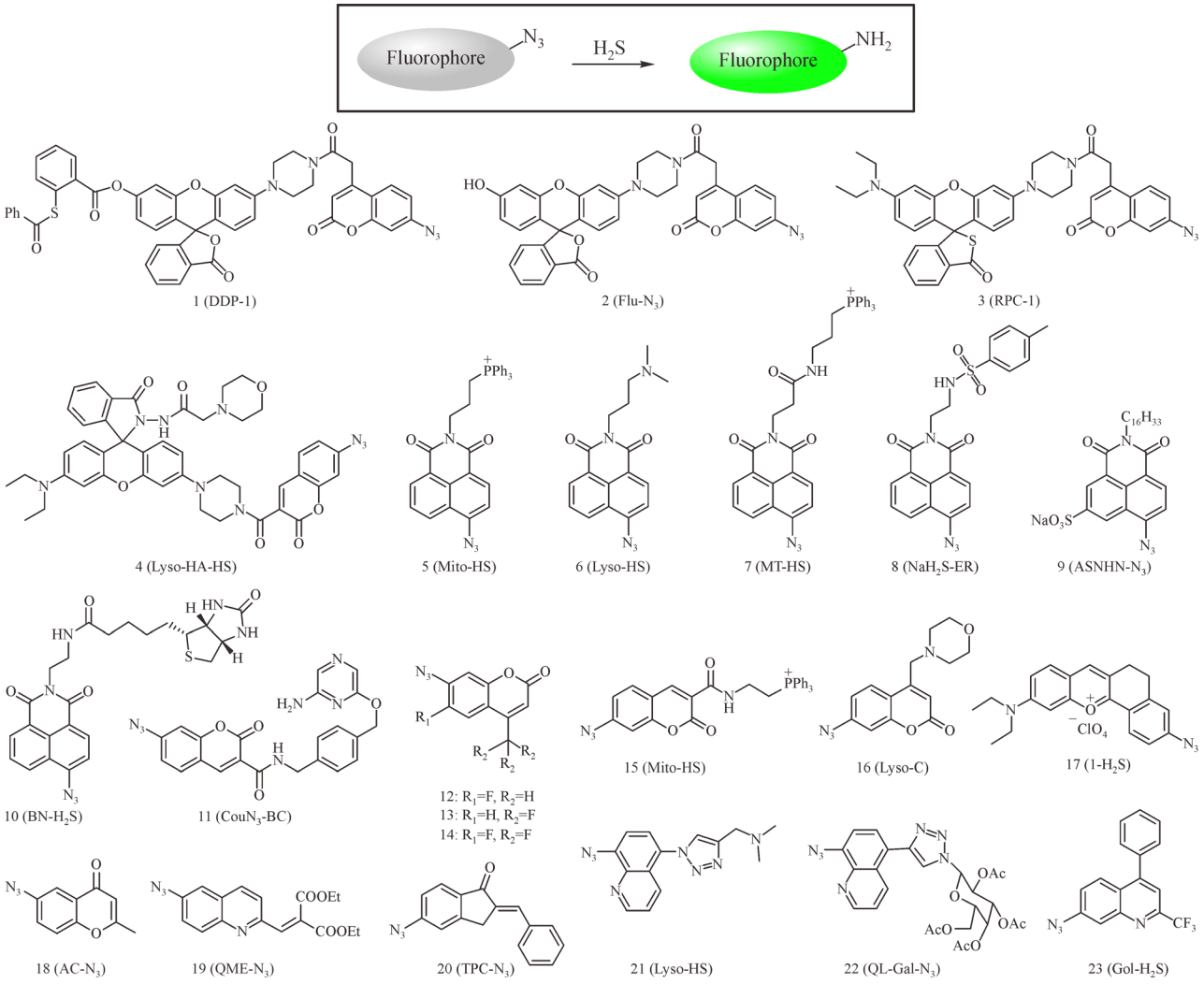

Fig. 1 Chemical structure of azide-based probes 1–23.

to its low toxicity and good cell membrane permeability, probe 25 can identify endogenous and exogenous H_2S in living cells. Chemical structures of nitro-based probes are shown in Fig. 2.

3.3 Probes based on reduction of azo and hydroxamino group for sensing

In previous studies, probes utilizing the redox property of hydroxamino group and the azo group have been developed. In 2014, Li et al. reported probes 26–32 (azo1–azo7), which realized "off-on" fluorescence via reduction of the azo group for sensing H_2S [45]. Probe 28 (azo3) carrying a pentafluorobenzyl group, had a 22-fold increasing selectivity towards H_2S over other species and had a detection limit of 500 $nmol \cdot L^{-1}$. The data described above illustrated that utilization of a nitrogen atom redox state is an ideal and available method for designing fluorescent probes. In 2017, Chen et al. developed an excited-state intramolecular proton transfer (ESIPT)-based fluorescent probe 33 (PHS1) to sense H_2S [46]. A hydroxylamine group was utilized as the H_2S reporter, which was based on the fact that hydroxylamine can be reduced by H_2S to form the corresponding amine group. Hydroxylamine as a protecting group of 3-amine nitrogen caused no emission of the fluorophore via preventing the ESIPT process until it was specifically reduced by H_2S. Chemical structures of azo-based and hydroxamino-based probes are shown in Fig. 2.

4 Nucleophilicity-based fluorescent probes

In addition to the reductive property, H_2S itself also possesses much stronger nucleophilicity than other thiols, which is due to its smaller size and lower p*K*a [47]. Such properties provide the possibility and availability to design fluorescent probes via a specific reaction between probes and H_2S. Based on these properties, a lot type of specific reactions have been exploited for the development of probes, such as the cleavage of DNP group after nucleophilic reaction, H_2S-induced S–S cleavage followed by intramolecular nucleophilic reaction, bringing great diversity and practicality to the family of fluorescent probes for H_2S detection.

4.1 Probes based on substitution of chloride atom for sensing

Chloride is a latent site, which can be nucleophilically substituted by H_2S, leading to changes in fluorescence intensity. Based on this, Montoya et al. developed an nitrobenzofurazan (NBD)-based colorimetric probe 34 [48]. However, the selectivity against biothiols, such as GSH and Cys was not as expected. In 2014, Han's group reported an "on-off" cyanine-based a NIR probe 35 that could be utilized to selectively detect H_2S in serum with a low detection limit in living cells [49]. Unfortunately, they did not screen for the selectivity of the probe. Inspired by

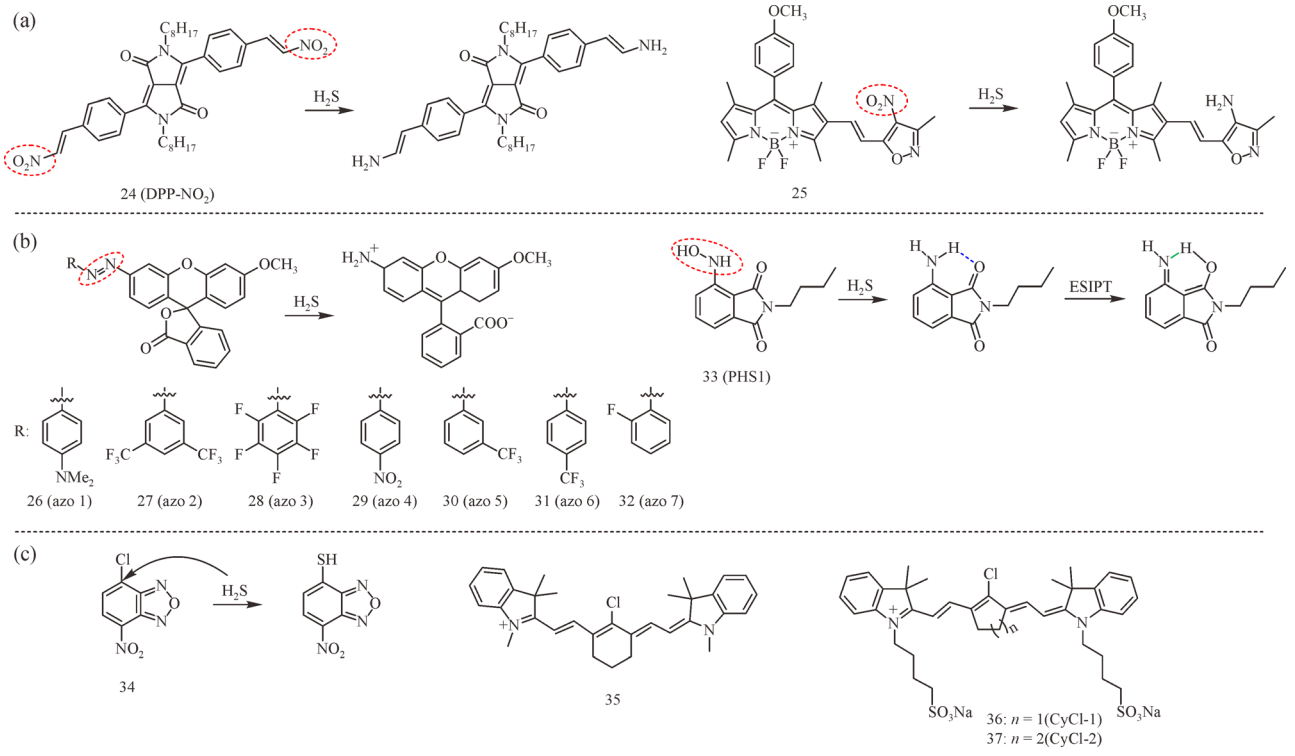

Fig. 2 (a) chemical structures of nitro-based probes 24 and 25; (b) chemical structures of azo-based and hydroxamino-based probes 26–33; (c) chemical structures of probes 34–37.

Han's work, Li et al. reported on probes 36 (CyCl-1) and 37 (CyCl-2), which could perform photoacoustic imaging of H_2S in living mice [50]. The chemical structures of probes 34–37 are presented in Fig. 2.

4.2 Probes based on breakage of conjugated systems for sensing

As universally recognized, H_2S, a good nucleophile, can attack the electrophilic center of fluorescent molecules and break the conjugate system. Probe 38 (BH-HS) was developed based on this mechanism, performing great fluorescent imaging ability towards both intracellular and exogenous H_2S [51]. In brief, BODIPY was selected as the fluorescence reporting group, with dimethyl amine as the electron donor and hemicyanine as recognition site for H_2S. Thereafter, Feng et al. developed a ratiometric Förster resonance energy transfer (FRET)-based probe 39 (CPC) that integrated coumarin with hemicyanine [52]. Due to the nature of hemicyanine, probes 38 (BH-HS) and 39 (CPC) both demonstrated preferential distribution in mitochondria with excellent reaction kinetics with H_2S, which enabled reaching a maximum fluorescence within several minutes. Taking hemicyanine as a H_2S trigger, Liu et al. established an internal charge transfer (ICT)-based probe 40 (TP-PMVC) for tracking the H_2S inside the lysosomes [53]. Two active sites (pyridine and hemicine) were included in the structure to react with H^+ and H_2S, respectively. The pyridine part with its appreciable p*K*a (≈5.0) was selected as the H^+ site and lysosomal targeting unit. These innovations allowed for simultaneous screening of lysosomes and lysosomal H_2S with double-color imaging. Moreover, based on the FRET mechanism, they introduced a H_2S probe 41 (CP-H_2S) with favorable colorimetric and ratiometric fluorescence, which selected the pyronine dye and coumarin chromophore as the energy acceptor and the energy donor, respectively [54]. In an aqueous solution, through the FRET process, probe 41 (CP-H_2S) showed intrinsic red emission of the pyronine unit, while the presence of H_2S inhibited the FRET process and resulted in blue emission from the coumarin part, while the red emission was reduced. Therefore, probe 41 (CP-H_2S) was promising in living cell imaging.

In 2017, based on ICT, a concise and efficient fluorescent probe 42 (Mi) was synthesized [55]. Probe 42 (Mi) can be used to detect H_2S with the naked-eye. Li et al. successfully applied probe 42 (Mi) to determine H_2S on agar gels with satisfactory results. These results indicated that probe 42 (Mi) performed a promising application of H_2S sensing in environmental samples. Compared with probe 42 (Mi), Ma et al. focused on improving reaction sensitivity. In 2018, they reported a ratiometric fluorescent probe 43 (CyT) of which its hemicyanine part selectively reacted with H_2S in the mitochondria of living cells [56]. Moreover, this probe showed low toxicity to HeLa cells and had a good imaging effect in living cells and zebrafish. Except for traditional fluorophores with aggregation-caused quenching property, AIE luminogens (AIEgen) also received extensive attention. Its outstanding optical properties facilitated its application on biological imaging and sensing. Taking these factors into account, Ma et al. reported an AIEgen probe that was positively charged [57]. Probe 44 (Indo-TPE-Indo) with two indolium groups provided more opportunities to target mitochondria and had better responses to H_2S in cells. Thus, as well as being applied for the detection of H_2S *in vivo*, such as H_2S in cancer cells and tumors, probe 44 (Indo-TPE-Indo) could function to visualize the H_2S diversity in mitochondria of living cells. As mentioned above, the generation of H_2S is related to enzyme CSE and CBS. In previous studies, it was confirmed that the CBS gene in humans is located on chromosome 21. Thus, enzyme CSE could produce H_2S, and CBS is in close connection with RNA. To better understand the function of RNA, Liu et al. developed probe 45 (TP-MIVC), which was considered the first paradigm of probes capable for simultaneously reporting RNA and H_2S with clear fluorescence signals [58]. Two different sites (carbazole and indolenium) respectively reacting with RNA and H_2S of this probe created versatile imaging properties. In cancer cells, zebrafish, and living animals, probe 45 (TP-MIVC) performed clear fluorescence imaging of RNA and H_2S. It is worth noting that by observing fluorescence intensity, it was found that probe 45 (TP-MIVC) distinguished tumor mice from normal mice. Chemical structures of probes 38–45 are shown in Fig. 3.

This type of probe was often used for developing the ratiometric H_2S probes, which change the fluorescence emission by destroying the conjugate system. However, this strategy may be affected by other nucleophilic biothiols.

4.3 Probes based on removal of DNP for sensing

DNP is an extremely strong electron-withdrawing group and can lead to fluorescence quenching after being attached to fluorophores due to its strong electron absorption performance. The C–O bond between DNP and fluorophores is easy to be cleaved after nucleophilically attacking by H_2S, with fluorescence turned on afterwards. The characteristics mentioned above make DNP an ideal group for engineering reaction-based probes for H_2S. Obviously, incorporation of the DNP functional group onto different fluorophore scaffolds could yield in fruitful innovations of probes for H_2S. For example, by uniting coumarin with benzothiazole, Cui et al. synthesized fluorescent probe 46 (CTN) for H_2S based on thiolysis of the dinitrophenyl ether moiety [59]. By taking hemicyanine dye as the NIR skeleton, Zhang et al. developed NIR probe 47 (NIR-HS), which allowed for imaging and tracking H_2S *in vivo* [60]. In 2017, Tang's group successfully developed the first self-assembled fluorescent

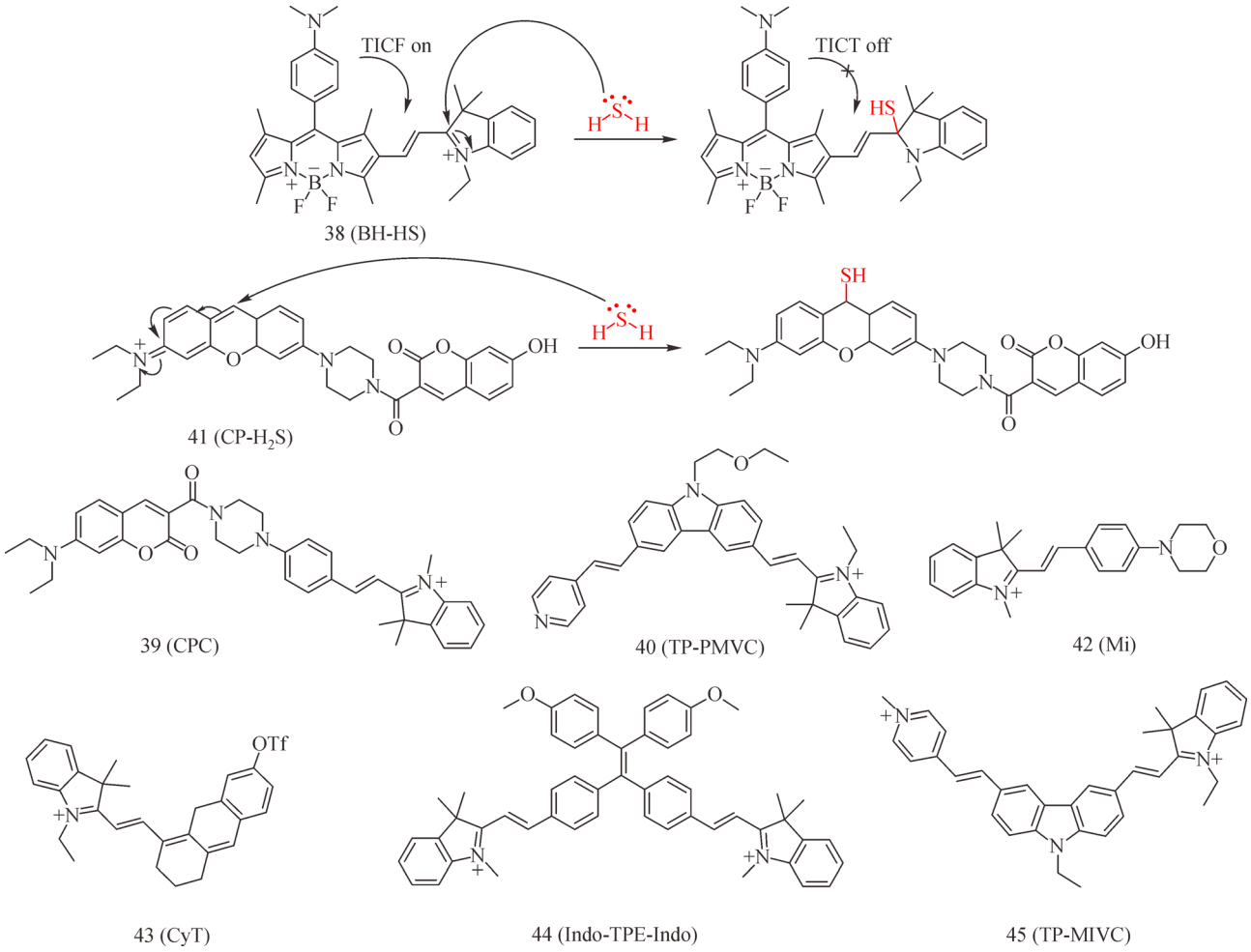

Fig. 3 Chemical structures of probes 38–45.

nanoprobe 48 (TPE-3) with both AIE and ESIPT characteristics to detect H_2S through a modified nanoprecipitation [61]. Moreover, nanoprobe 48 (TPE-3) could be used for H_2S imaging in live cells and *in vivo* due to its excellent water dispersibility and good biocompatibility. It is well known that two-photon-excited bioimaging has been widely utilized because of its deeper tissue penetration. Herein, Zhou et al. designed an efficient two-photon mitochondria-targeting dye 49 (TP-NIR-HS) with a H_2S recognition moiety [62]. As expected, probe 49 (TP-NIR-HS) was essentially non-fluorescent, which might be ascribed to the ICT effect by the strong electron-withdrawing DNB group. Release of the fluorophore was the result of the addition of H_2S, which caused the cracked portion of DNB to be left behind and turned on the fluorescent signals. Subsequently, probe 49 (TP-NIR-HS) was applied to imaging living cells and tissues, resulting in high imaging resolution and a deep-tissue imaging. The effect of pH on the sensitivity of probe 49 (TP-NIR-HS) is unknown.

In 2018, Gu et al. synthetized fluorescent probe 50 (2-CHO-OH) with DNP as the H_2S reporter and an adjacent aldehyde group to improve sensing performances [63]. The strategy was also employed by Qian et al., who designed a NIR fluorescent probe 51 (NDCM-2) [64]. The mechanism was as follows. H_2S nucleophilically added to the aldehyde group, resulting in a hemiactal, which promoted the intramolecular thiolysis process of the 2,4-dinitrophenyl ether. Based on the photoinduced electron transfer (PET) theory, Chen et al. developed a fluorescence probe 52 (NIPY-DNP) for H_2S [65]. Later, Ji et al. reported a long wavelength fluorescent probe 53 (TMSDNPOB) based on the BODIPY structure to detect H_2S [66]. The fluorescence signal of the probe was significantly enhanced after the sensing reaction. Starting with probe 49 and with the intention to overcome the shortcomings of a complex synthesis process and short emission wavelength, Li et al. obtained a long-wavelength probe 54 (LC-H_2S) after only two synthesis steps [67]. Unfortunately, compared to probe 49, probe 54 (LC-H_2S) was not a two-photon fluorescent probe. Chromone derivatives have also been used as fluorophores. Liu et al. designed a turn-on fluorescent 55 (A) for H_2S detection, which was based on an ESIPT process [68]. Bearing the classical morpholine as a

lysosome targetable marker, Wu et al. obtained a novel lysosome-targeting probe 56 (DMC) [69]. Moreover, coumarin had been adopted to load the DNP. Yang et al. reported a molecular probe 57 (Cda-DNP), which could access all compartments in the cell that detect H_2S in cells and living animals [70]. Probe 57 (Cda-DNP) consisted of three functional domains: a H_2S sensing domain, a fluorescence domain, and a biomembrane penetration domain. Moreover, the lateral chain *N*,*N*-dimethylethylenediamine played a significant role in enabling probe 57 (Cda-DNP) to enter cells and penetrate into different organelles.

Sun et al. developed a new molecular probe 58 (NR-NO_2) taking benzothiazole-xanthene dyad as the fluorophore unit [71]. This probe not only tracked and analyzed H_2S in mitochondria, but could also observe a mouse liver injury model caused by overdose of metformin via detecting hepatic H_2S. The tracking and analysis of H_2S in mitochondria was of great significance. Thus, Zhao et al. developed a mitochondria-targeting fluorescent probe 59 (Mito-NIR-SH) by introducing DNP into a Changsha NIR fluorophore, which was used to detect intracellular H_2S [72]. Together, the experimental results demonstrated that 59 (Mito-NIR-SH) could selectively target mitochondria and image exogenously and endogenously H_2S in the cellular environment. It is often effective to improve probe properties by modifying fluorophores. Using this rationale, Zhu et al. synthesized two different probes, by introducing methoxy groups on the BODIPY 3,5-positions, and designed and synthesized probes with large Stokes shift for detecting H_2S [73]. Probe 60 (DMOEPB) had a dinitrophenyl ether as the reactive moiety and probe 61 (DMONPB) had a nitro group as a reactive group for H_2S. In addition, based on BODIPY, Fang et al. obtained a naked-eye and "on-off" fluorescent probe 62 for detecting H_2S [74]. The colorimetric sensing ability of this probe facilitated naked eye detection, thereby overcoming some drawbacks, such as probe concentration, sample environment and light scattering. Utilizing NIR dye cyanine as the fluorophore, Su et al. and Lin et al. developed probes 63 and 64 (QCy7-HS), respectively [75,76]. Due to blockage of the twisting of the *N*,*N*-diethylamino group at the fluorophore, Zhang et al. synthesized H_2S probe 65 (Z1) with the functions of naked-eye colorimetry and efficient ER localization [77]. Moreover, Zhong et al. used 4-diethylaminosalicylaldehyde and 1,4-dimethylpyridinium iodide as synthetic raw materials and synthesized probe 66 (L) by a two-step reaction via eliminating d-PET and recovering ICT processes to identify H_2S [78]. Chemical structures of DNP-based probes 46–66 are shown in Fig. 4.

4.4 Probes based on removal of NBD group for sensing

Similar to the hydrolysis of DNP ether by H_2S, a NBD group has also been widely used as a H_2S-probe trigger for its fluorescence-quenching nature and easily-leaving property after nucleophilic reaction with H_2S. Based on this, in 2016, Ding et al. reported a remarkably simple probe 67, which had fast fluorescence responses for all mercaptans [79]. Nevertheless, probe 67, like many other NBD ether-based probes, could not selectively detect H_2S in the presence of other biological thiols. To solve this problem, their research team reported that the introduction of an aldehyde group on probe 67 resulted in highly selective H_2S probes 68 and 69, both of which detected H_2S in the presence of other biological thiols [80]. By attaching NBD to fluorescein and rhodamine dyes through a piperazine linker, Wang et al. obtained probe 70 and a NIR probe 71 [81]. Probe 71 showed a higher reaction rate toward H_2S, which might be attributable to the positively-charged nitrogen in rhodamine and mitochondrial targeting. Enlightened by Grimm et al. [82], Ismail et al. rationally designed and synthesized a novel azetidinyl-rhodamine-NBD dyad 72 that quickly detected H_2S in the range of infrared [83]. Compared to 71, obstructing the twisting amino side chain dramatically enhanced the performance of probe 72. Furthermore, Wei et al. developed the first H_2S-specific fluorescence probe 73 based on the cleavage of NBD [84]. Later, their group designed a julolidine-fused coumarin-NBD probe 74 that allowed for the detection of H_2S with improved performance [85]. Probe 74 showed excellent sensing performances with green-light emitting and was successfully used for biological imaging in cells and in zebrafish. In addition, Huang et al. developed an NBD-based fluorescent probe 75 based on a click reaction of alkyne-containing NBD derivative and azidocoumarin [86]. By choosing classical coumarin dye as the fluorophore, Zhang et al. prepared a fluorescent probe 76 (ER-CN) for sensing H_2S by bearing a methyl sulfonamide group as an ER targetable marker [87].

Triphenylphosphonium can be used as the anchoring part for mitochondria, allowing it to enter mitochondria for selective monitoring and imaging. Therefore, Pak et al. engineered a mitochondria-target probe 77 with triphenylphosphonium as a mitochondria-oriented marker [88]. Utilizing 3-hydroxyflavone as fluorophore instead, Hou et al. developed a colorimetric and fluorescent dual probe 78 for H_2S due to the color and fluorescence induced by the interaction of probe with H_2S [89]. In 2017, two BODIPY-NBD based fluorescent probes namely 79 (BDP-N1) and 80 (BDP-N2) were prepared by integrating the styryl-BODIPY fluorophore with the NBD moiety using a one-pot reaction [90]. They were both fluorescence-off due to the quenching effect from the NBD group. Thiolysis was induced after introducing HS^-, which made it exhibit off-on fluorescent signal. Zhang et al. obtained a long wavelength NIR fluorescent probe 81 based on BODIPY and carrying an NBD moiety, which linked with the benzyl pyridinium moiety through ether linkage at the meso

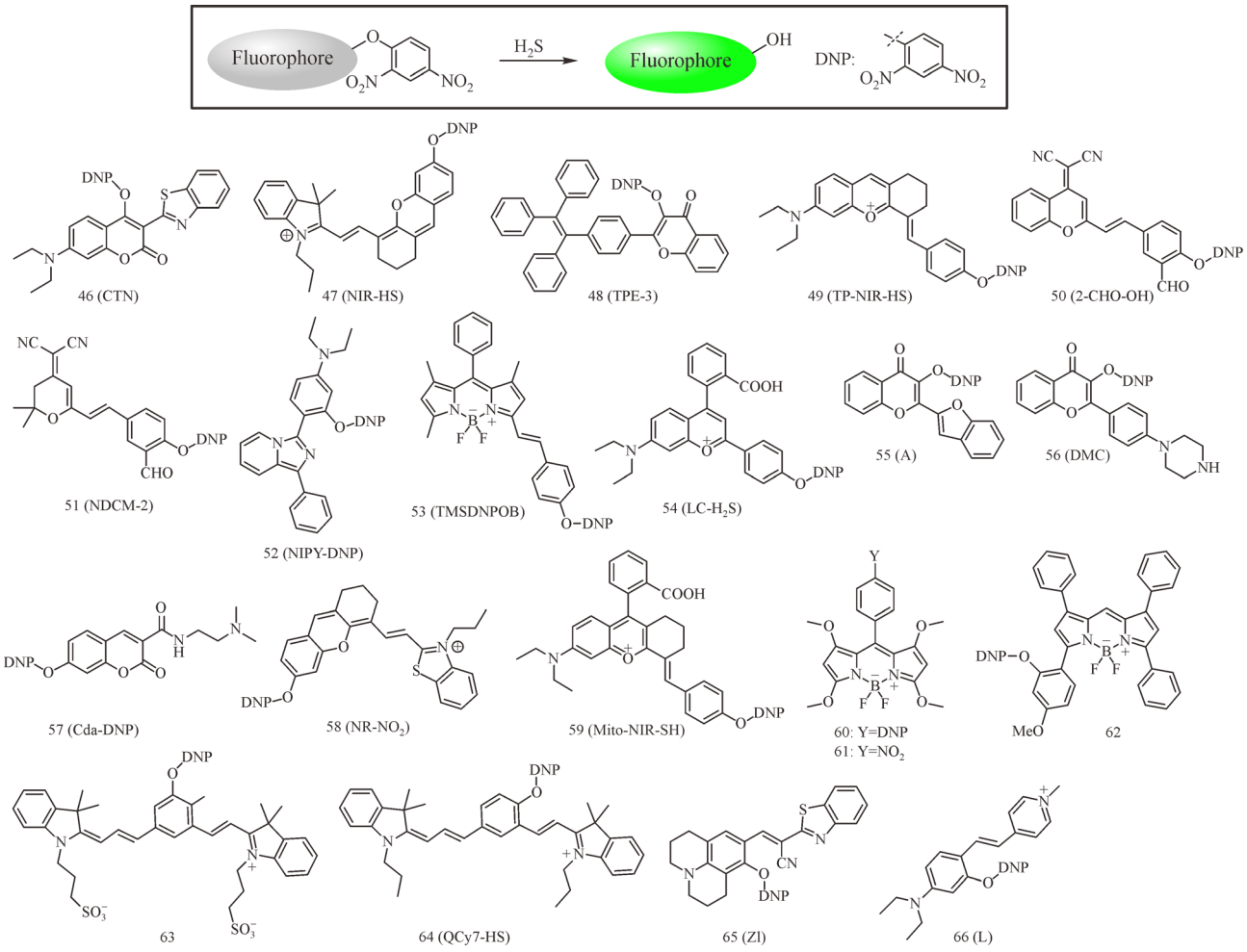

Fig. 4 Chemical structures of DNP-based probes 46–66.

position [91]. It simultaneously displayed distinct responses to H_2S/GSH and Cys/Hcy from visible/NIR dual emission channels. Inspired by the pioneer's work, through integration of an NBD amine reaction group into rhodamine fluorophore, Wang et al. presented an "off-on" fluorescent probe 82 for H_2S [92]. In 2018, taking cyanine dye as NIR skeleton, Xiong et al. developed a NIR fluorescent probe 83 (NIR-H_2S) based on a thiolysis reaction for H_2S detection, which successfully monitored H_2S in cells and mice [93]. So far, a large number of fluorescent probes for sensing H_2S have been developed. However, all H_2S probes based on NBD exhibited single photon excitation responses. Because of this kind of probe short excitation light, it sometimes had problems for biological imaging, especially for tissue imaging. On the contrary, two-photon probes can solve the above-mentioned problem. Tang and Jiang reported a two-photon fluorescent probe 84 (L) utilizing the FRET strategy [94]. Probe 84 (L) was employed to image exogenous and endogenous H_2S in living cells. Chemical structures of NBD-based probes 67–84 are shown in Fig. 5.

4.5 Probes based on nitro or azide reduction-triggered self-immolation

Reduction of the azide or nitro group to amino followed by a self-immolative reaction to liberate free fluorophores, has been utilized to design reaction-based H_2S fluorescent probes. Inspired by hypoxia pro-drug moiety the *p*-nitrobenzyl group, Qian'group developed ratiometric probe 85 (RHP) for hypoxia in 2011 [95]. Inspired by Qian' work, Zhang et al. developed probe 86 (RHP-2) in 2014 [96]. Simultaneously, the tandem reaction mechanism was successfully confirmed by Cui et al. Based on this mechanism, Zhang et al. developed probe 87, which could be reduced by H_2S, and proceeded intramolecular cyclization after removal of the *p*-aminobenzyl group to construct a renascent fluorophore [97]. Most reported probes of this type only responded to H_2S with fluorescence intensity (based on the "turn on" or "turn off" mode) which was significantly affected by complex factors, such as the detection environment and probe location. Wang et al. developed a naphthalimide-based colorimetric and

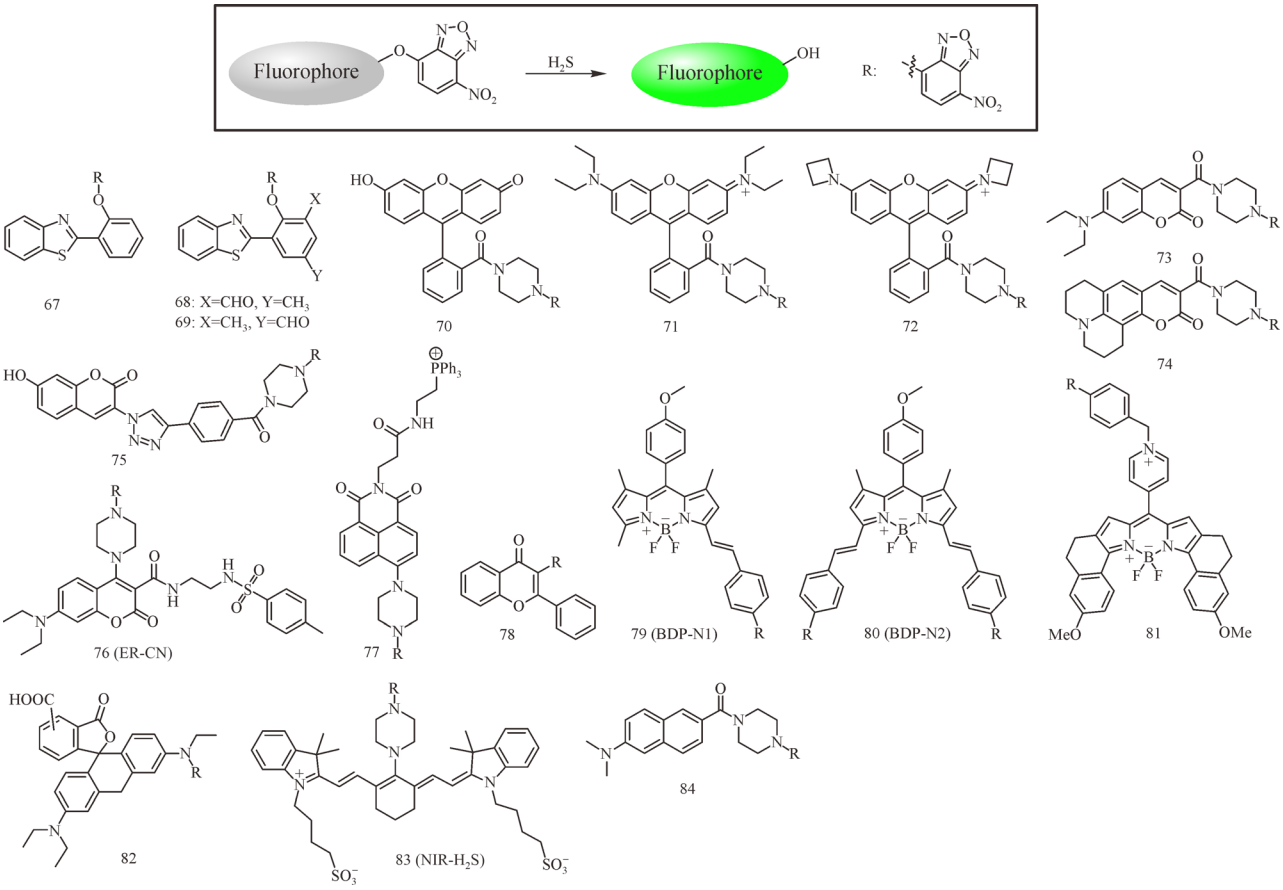

Fig. 5 Chemical structures of NBD-based probes 67–84.

ratiometric fluorescent probe 88 (NS1) [98]. The azide portion of the probe was specifically reduced by H_2S, and underwent a spontaneous 1,6-elimination reaction to form naphthimide compounds, which in turn exhibited strong fluorescence. This process resulted in a larger shift of the emission spectrum to achieve the colorimetric and ratiometric fluorescence response to H_2S. Later, a novel strategy was developed by Steiger et al. for H_2S based on the self-immolation of benzyl thiocarbamates to release carbonyl sulfide, which was quickly converted into H_2S by carbonic anhydrase. Importantly, this strategy provided solutions to key challenges associated with both H_2S delivery and detection. Finally, they designed and synthesized fluorescent probe 89 (MeRho-TCA) and confirmed triggering the release of H_2S [99].

In 2017, by introducing the classical morpholine as a lysosome targetable marker, Feng et al. prepared a ratiometric double-photon fluorescent probe 90 (LR-H_2S) for imaging lysosomal H_2S [100]. Furthermore, Thirumalaivasan et al. obtained probe 91 (PyN_3) based on pyrene [101]. By reducing the azide to an amine and self-immolative cleavage of the *p*-aminobenzyl group in the molecule, the fluorophore was released. What's more, Park et al. obtained a new type of NIR probe 92 (NIR-Az) for H_2S determination [102]. Probe 92 (NIR-Az) had a high selectivity for H_2S among the 16 analytes tested including common reducing agents. Utilizing the excellent biocompatibility and rapid cell internalization of probe 92 (NIR-Az), Park et al. successfully proved its useful ability to monitor the concentration and time-dependent changes of H_2S in living cells and animal aspect.

In 2018, a dual-response fluorescent probe 93 (Mito-VS) was designed and synthesized by Li's group to monitor the level of viscosity and H_2S, respectively [103]. Probe 93 (Mito-VS) was non-fluorescent due to a free intramolecular rotation between dimethylaniline and pyridine. After an increase in viscosity, rotation was prohibited and an intense red fluorescence was released. Upon the addition of H_2S, probes reacted with H_2S and a strong green fluorescence was observed. Utilizing the same principle, Yin's group synthesized another BODIPY fluorescent probe 94 (BDP-N_3), which had viscosity sensitivity and detected H_2S with high selectivity [104]. Those probes allowed for the detection of both H_2S and viscosity in a biological system. In 2019, due to the PET between fluorophore and azido moiety by a carbonate linker, Zhou et al. presented an "off-on" mitochondria-targeted NIR probe 95 (Mito-N_3) [105]. Simultaneously, Yang et al. developed an interesting red-

emitting fluorescent probe 96 [106]. Upon the addition of H_2S, the reduction of the azido group generated an amino derivative, which rapidly released an imine intermediate and subsequently went through an intramolecular cyclization to release fluorescence. In addition, by introducing a self-immolative group to achieve a lower detection limit, Zhu et al. obtained a rhodamine-based probe 97 (MF-N_3) that selectively accumulated in lysosomes and presented turn-on fluorescence when H_2S and protons were present at the same time [107]. Chemical structures of probes 85–97 are shown in Fig. 6.

4.6 Probes based on electrophilic cleavage-triggered intramolecular tandem reactions

Due to the dual-nucleophilicity of H_2S, a new tandem reaction between disulfide and H_2S was discovered. This tandem reaction started with the nucleophilic substitution between disulfide and H_2S. Successively, intramolecular cyclization between the freshly produced thiol and ester occurred, with simultaneous fluorophore release. Inspired by this tandem reaction, Li et al. selected 3-hydroxyflavone as the fluorophore and 2-(pyridine-2-yl-disulfanyl)benzoic acid as the H_2S reporter, yielding fluorescent probe 98 (HF-PBA). Probe 98 (HF-PBA) became a potential multifunctional fluorescent probe, because it could also distinguish H_2S and biothiol through different fluorescence bands [108]. In 2017, a water-soluble fluorescent probe 99 (HS-1) was prepared by integrating the 4-hydroxycoumarin fluorophore with a disulfide moiety by Yin's group [109]. The reaction between probe 99 (HS-1) and H_2S triggered the cleavage of the disulfide bond and subsequent intramolecular cyclization, thereby releasing 4-hydroxycoumarin, resulting in a ratio fluorescence response. Other relevant thiols induced no observable fluorescent response. In 2018, utilizing excellent properties of dicyanomethylene-4H-pyran as fluorophore, Men et al. rationally prepared a specific fluorescent probe 100 (DCM-PBA) by integrating PBA fragment to dicyanomethylene-4H-pyran via ester bridge [110]. Moreover, based on a semiheptamethine derivative, a classic NIR dye scaffold, Zhang et al. developed a fluorescent probe 101 (Cy-PBA) with NIR fluorescence emission [111]. In 2019, using the same strategy, a ratiometric-visualized fluorescent probe 102 was reported [112].

Similar to the above-mentioned mechanisms, Wang et al. introduced a colorimetric fluorescence probe 103 based on cyanine, allowing for the detection of H_2S sensitively

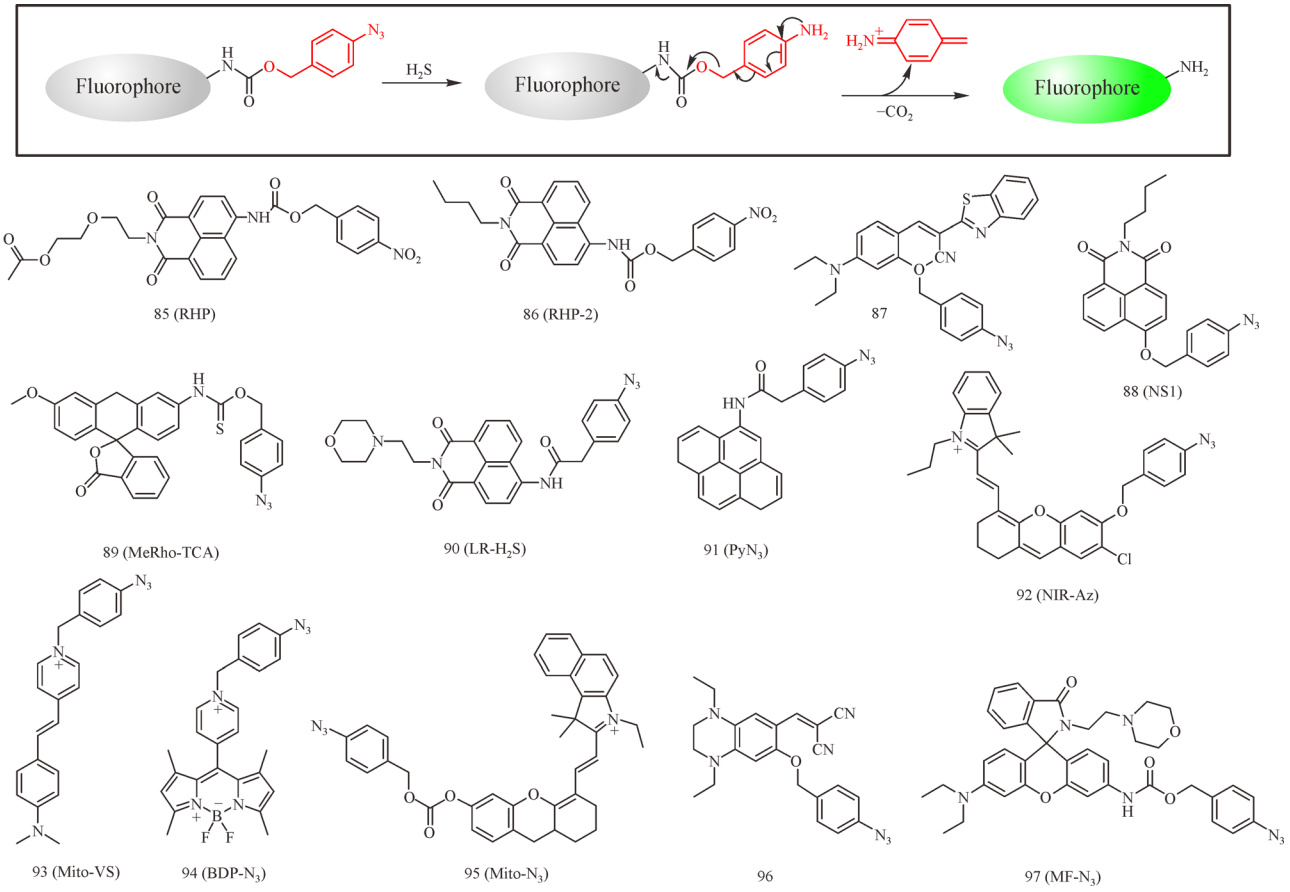

Fig. 6 Chemical structures of probes 85–97.

and selectively [113]. Nucleophilic attack of the disulfide bond by H_2S led to cleavage of the disulfide bond and an intramolecular cyclization to promote release of the fluorophore, as detected through the enhancement of the fluorescence signal and color change of the reaction mixture. In addition, utilizing the same strategy, Wang et al. designed and synthesized fluorescence probe 104 (DCN-S) for H_2S detection [114]. The disulfide bond of probe 104 (DCN-S) was broken under the nucleophilic substitution of H_2S followed by the generation of dicyanoisophorone derivative, which emitted an orange fluorescence. Furthermore, the diselenide bond is about 5 orders of magnitude faster to be cleaved by H_2S than the disulfide bond. Obviously, the diselenide group represents an ideal candidate for designing probes that respond quickly to H_2S. Based on this rationale, Guan et al. reported a double-switch mechanism for fluorescence probe 105 (HBTSeSe) of sensing H_2S employing a diselenide bond [115]. Chemical structures of probes 98–105 are shown in Fig. 7.

4.7 Employing tandem reaction with proximal aldehyde and α,β-unsaturated carbonyl group for sensing H_2S

Utilization of a proximal aldehyde group and α,β-unsaturated carbonyl group as a trapping moiety, another novel tandem reaction was developed. It was due to the dual-nucleophilicity of H_2S that can lead to a sequential Michael-addition reaction with an aldehyde group and an α,β-unsaturated carbonyl successively. Qian et al. first designed two probes 106 (SFP-1) and 107 (SFP-2), which showed 50 to 100-fold selectivity against other biothiols, including GSH, Cys and the like [116]. In 2013, Li et al. developed an ICT-based probe 108 (ZS1) [117]. This probe possessed an incredibly over 5000-fold selectivity against biothiols. Moreover, inspired by this mechanism, Singha et al. developed three probes 109 (P1), 110 (P2), and 111 (P3) [118]. To enrich the electronic density of benzene by adding methoxy groups, high selectivity towards H_2S over Cys was achieved. At higher pH values, a new HO^--condensation between an enolate and an aldehyde has been

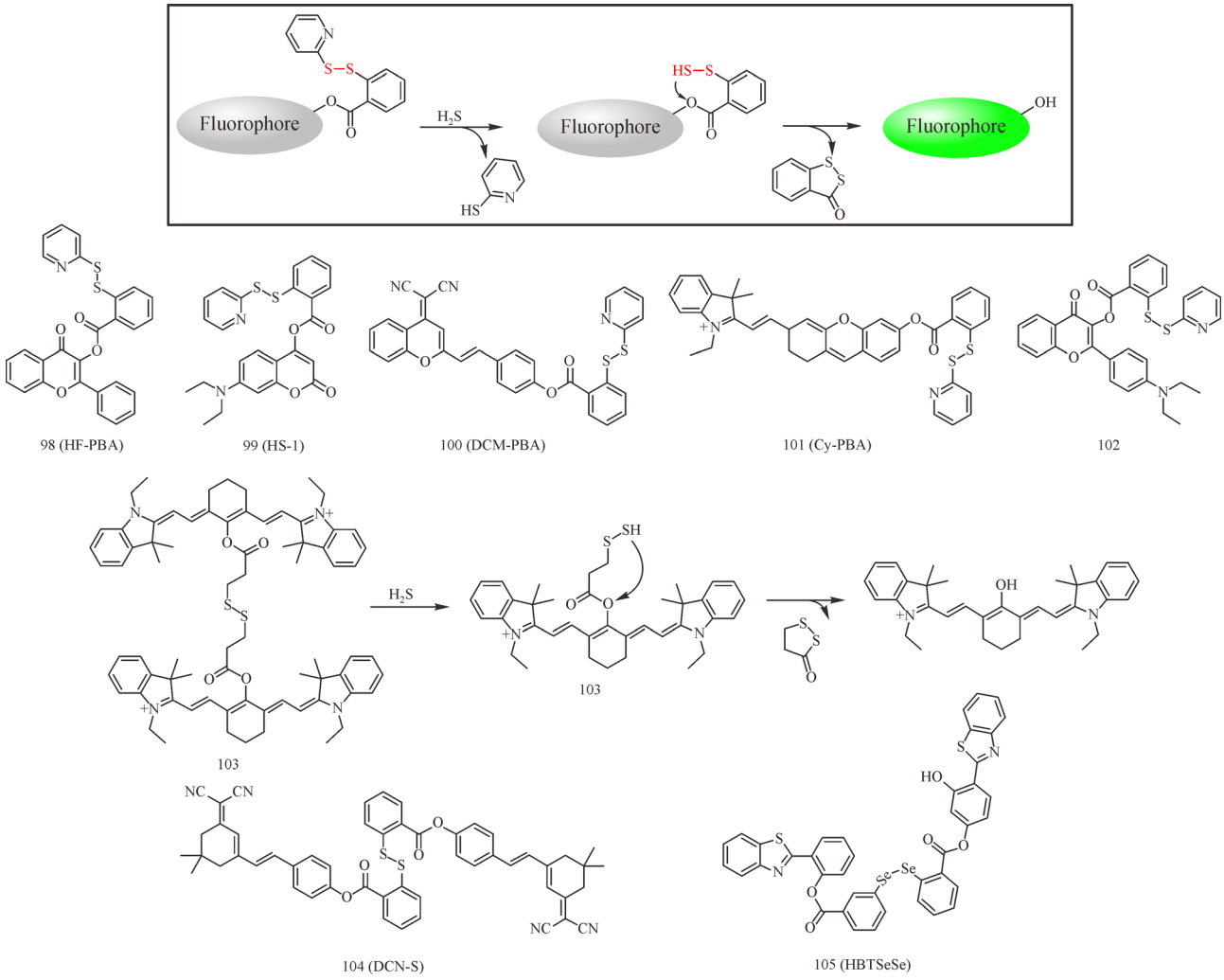

Fig. 7 Chemical structures of probes 98–105.

revealed. Later, to develop a H_2S probe emitting in the longer wavelength region, preferably in the red or above (> 625 nm), Ryu et al. exploited an "acetyl-benzocoumarin" as the dye platform and developed probe 112 (P5) [119]. The reactivity of 112 (P5) toward H_2S was even faster than the previously-reported H_2S probe 111 (P3) that showed signal saturation after 8 min. Chemical structures of probes 106–112 are shown in Fig. 8.

4.8 Other types of fluorescent probes for H_2S

Other fluorescent probes not limited to the above-mentioned mechanisms for detecting H_2S have also been reported. Chen et al. developed three rhodamine-propargylic ester-based probes 113 (RB-PE-1), 114 (RB-PE-2), and 115 (RB-PE-3) [120]. Tandem reactions between H_2S and propargylic esters of rhodamine B(RB-Fes) led to spirocyclization of probes, rendering fluorescence off. Furthermore, an epoxide-based fluorescent probe 116 (FEPO-1) was developed by Chen's group [121]. After being attacked by H_2S at the C–O bond of epoxide, the epoxide ring opens and leads to alteration of the conjugation system of the probe. Karakus et al. was the first to use electrophilic cyanate as the H_2S recognition group, and developed fluorescent probe 117 (FLVN-OCN) for H_2S by modifying the fluorescent dye based on ESIPT [122]. In the presence of reactive sulfur species, they expected that the oxygen-nitrile bond of the pre-fluorescent dye 117 (FLVN-OCN) would result in selective splitting and then release the free hydroxyl derivative of the fluorophore. As we all know, the second NIR window (NIR-II) probes had a greatly improved in spatial resolution and tissue penetration depth. Xu et al. rationally designed a dye 118 (ZX-NIR), which can generate the NIR-II emission after reacting with H_2S [123]. With the nanocomposites packaged, the designed nanoprobes had an excellent biocompatibility and good water solubility. This nanoprobe had a specific responsiveness to H_2S, so it can identify and image H_2S-rich colon cancer cells.

The well-known tetrazine structure was also used in fluorescence probes for detecting H_2S. Zhao et al. reported a novel reactive fluorescent probe for the selective detection of H_2S that adopted the Tz group and worked by the reduction of tetrazine to dihydio-tetrazine by H_2S. They next designed and synthesized three fluorescence probes with a tetrazine group, 119 (Coumarin-Tz), 120 (BODIPY-Tz-I), and 121 (BODIPY-Tz-II) [124]. In addition, a H_2S-induced deprotonation method would be another ideal strategy to design a probe because it has the advantage of non-interference with other thiols and a fast response time in physiological conditions. Utilizing this mechanism, Kaushik et al. reported a ratiometric colorimetric sensor 122 for the recognition of H_2S [125]. The reason for the change in ratio between spectrum and color was that H_2S induced the deprotonation of one of the –OH protons followed by changes of the resonance of probe 122. As is well known, many fluorescent probes are well-designed and can quickly and specifically respond to H_2S through addition reactions to break the conjugated π-system of C = C bonds. Based on this, Wang et al. reported a novel strategy using H_2S-mediated reduction of the C = C bond, which can effectively detect H_2S with turn-on dual-color fluorescence [126]. Here, they designed and synthesized probes 123 (PTZ-P1), 124 (PTZ-P2), 125 (PTZ-P3), and 126 (PTZ-P4), in which phenothiazine ethylidene malononitrile derivatives reacted with H_2S to form thiophene rings based on intramolecular cyclization reactions through reductive cleavage of C = C bonds. Of these probes, 126 (PTZ-P4) exhibited dual-color fluorescence after reductive cleavage.

Based on various types of reactions between H_2S and other chemical species, a large number of reaction-based probes were obtained. Due to the feasibility and diversity, reaction-based strategy has become the most widely applied strategy. However, emphasis is still needed regarding the discovery and elucidation of novel reaction

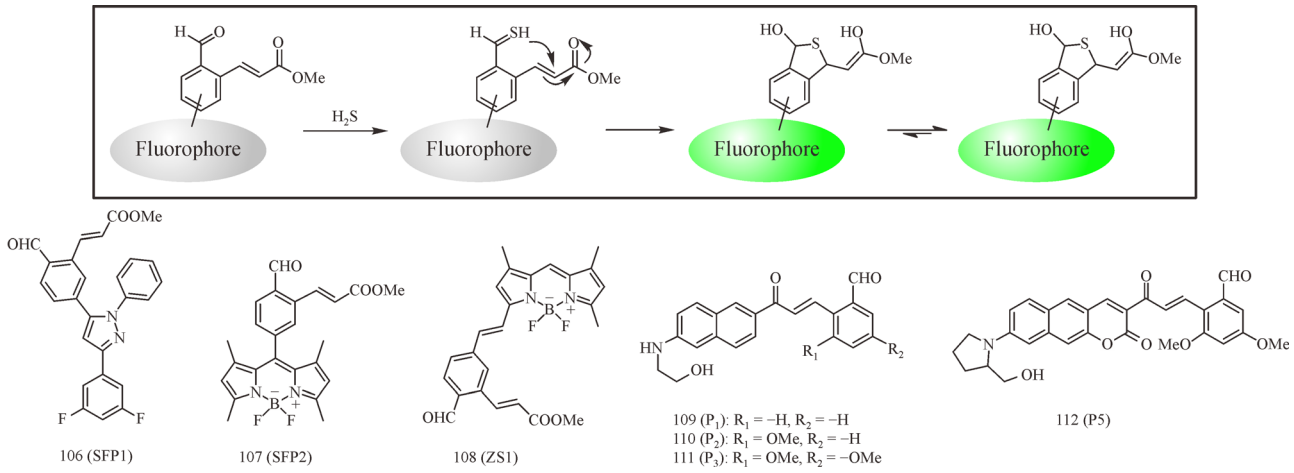

Fig. 8 Chemical structures of probes 106–112.

mechanisms, which are of better reaction kinetics and have a higher specificity. In addition, further modifications and improvements on available fluorescent probes should be promoted, in order to gain probes that are more compatible with the living system. Chemical structures of probes 113–126 are shown in Fig. 9.

5 Metal sulfide precipitation-based fluorescent probes for labeling H_2S

The reaction between Cu(II) and S^{2-}, generating CuS precipitate with K_{sp} about 10^{-45} (25 °C in water), has obtained broad utilization upon the design of fluorescent probes for detecting H_2S. Underlying this principle, Choi et al. reported the first CuS-based probe 127 in 2009, utilizing dipicolylamine (DPA) as the Cu(II) bonding moiety [127]. Similarly, with DPA as a Cu(II) bonding moiety, Hou et al. developed probe 128 [128]. The Cu(II) complex of the probe can be used to detect sulfide anions. In 2015, Yue et al. reported dinuclear Ru(II)-Cu(II) complex-based fluorescent probe 129, using DPA as the Cu(II) bonding moiety, which could detect H_2S in the rat brain [129]. In 2016, Lv et al. reported a fluorescent sensor 130 (CuHCD) that used hemicyanine-carbazole as the fluorophore and bipyridine-triazole-Cu^{2+} complex as the receptor, which selectively recognized HNO and H_2S respectively through the non-covalent modulation of surfactant assemblies [130].

Taking advantage of the stability of Cu(II) complexes formed with azamacrocyclic rings, Sasakura et al. developed four azamacrocyclic probes 131 (TACN), 132 (Cyclam), 133 (Hsip-1), and 134 (TMCyclen) [131]. Among those four probes, 133 (Hsip-1) revealed the best photophysical properties and detected sulfides in living cells. Wu et al. took 1,4,7,10-tetraazacyclododecane (cyclen) as the optimal fragment of 133 (Hsip-1) to develop two BODIPY-based NIR probes 135 and 136 in 2014, and realized H_2S imaging in living rats [132]. Also, in 2014, cyclen had been employed by Yuan's group to develop a dinuclear Ru(II)-Cu(II) complex-based fluorescent probe 137 [133]. This dinuclear complex possessed a large Stokes shift (159 nm) and had a sensitive response to H_2S (detection limit of 21.6 $nmol \cdot L^{-1}$). In 2015, Palanisamy et al. reported a mono anthracene functionalized cyclen fluorescent sensor MaT-cyclen forming complex 138 [Cu(MaT-cyclen)$_2$] with Cu(II) ions, which caused fluorescence quenching [134]. Complex 138 [Cu(MaT-cyclen)$_2$] acted as a fluorescent turn-on for H_2S by utilizing the displacement method.

Other single-ligand Cu(II) complex-based fluorescent probes were also developed. With 8-aminoquinoline as a Cu(II) bonding moiety via the piperazine ring linked to fluorophore, Cao et al. developed a cyanine-based NIR probe 139 [135]. Later, in 2012, Hou et al. reported a fluorescein-based probe 140 (L1Cu), utilizing 2-(8-hydroquinoline) acetohydrazide as the Cu(II) bonding moiety [136]. Shortly after the design of 140 (L1Cu), Hou et al. reported another fluorescein-based probe 141 (L1), utilizing 2-benzyl-acetohydrazide as the Cu(II) bonding moiety [137]. When 141 (L1) is compared with 140 (L1Cu), the former showed better fluorescent properties both in sensitivity and selectivity. Kar et al. reported FRET-based probes 142 (L-1) and 143 (L-2), utilizing indole as the energy donor and a xanthene-Cu(II) complex as the acceptor [138]. This probe could be used to detect both Cu(II) and sulfides, depending on the off-on response of the xanthene fluorophore corresponding to the occurrence of FRET by binding with Cu(II). In 2014, Tang et al. developed a benzimidazole-based probe 144 (L), carrying N-(2-hydroxyethyl)-piperazinegrcup as the Cu(II) bonding moiety [139]. Moreover, in 2015, Qian et al. obtained an *N*,

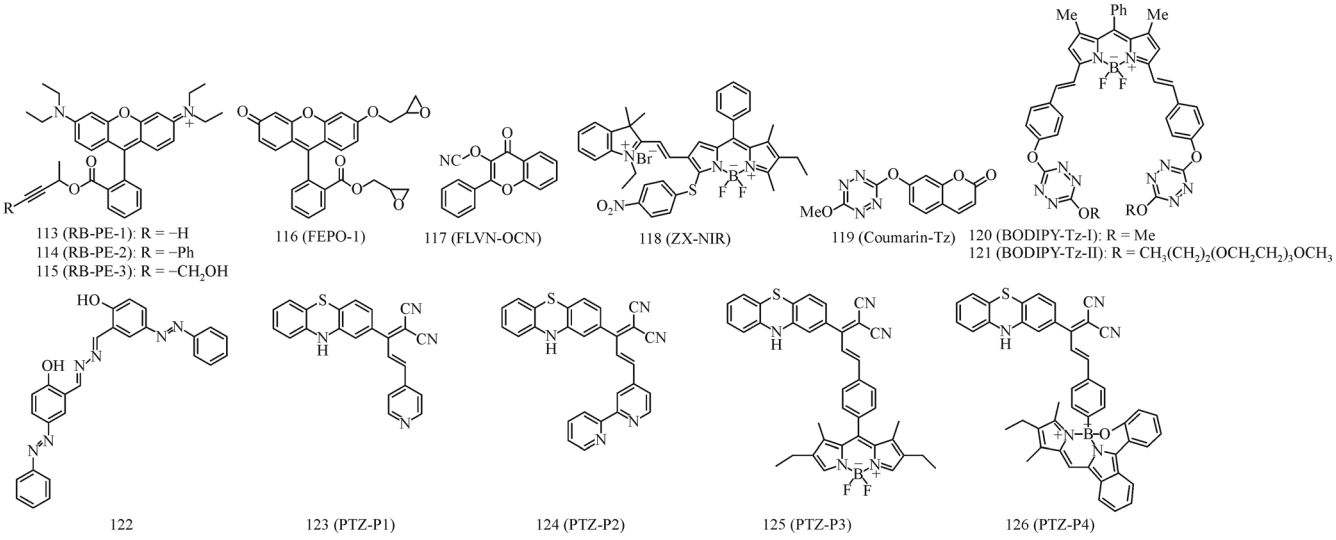

Fig. 9 Chemical structures of probes 113–126.

N-dimethyl naphthalene-based probe 145 (NJ1), bearing a 2-hydrazinylpyridine group as the Cu(II) bonding moiety [140]. Meng et al. furthered an NBD-based probe 146 (NL), utilizing salicyloylhydrazone as the Cu(II) binding moiety [141]. In 2015, Hai et al. reported a multifunctional pyridine-biquinoline-derivative probe 147, which was used to detect pyrophosphate and H_2S in aqueous buffer and cells [142]. By selectively coordinating with metal ions (Cu^{2+} and Zn^{2+} mentioned in article), fluorescence quenching occurred via PET. This metal complex reacted with both pyrophosphate and H_2S, resulting in the recovery of fluorescence. Through combining the triarylboron-fluorophore with cyclen and diphenylamine, Yang and coworkers developed three probes 148 (TAB-1), 149 (TAB-2), and 150 (TAB-3) [143]. Among these three probes, 148 (TAB-1) and 149 (TAB-2), bearing three and two cyclens, respectively, embodied a more suitable water solubility and cell permeability, and 149 (TAB-2) specifically had a mitochondria-target character. In 2016, a carbazole-based fluorescence probe was developed that presented an "on-off-on" type fluorescence response mode for sequential detection of Cu^{2+} and S^{2-}. High selectivity and sensitivity of probe responses to Cu^{2+} were barely affected by the coexistence of other interfering analytes. The subsequent addition of S^{2-} could effectively remove Cu^{2+} from the complex 151 (CAH-Cu^{2+}) to immediately recover the quenched fluorescence by releasing the free probe [144]. In 2017, Wang et al. reported a peptide ligand

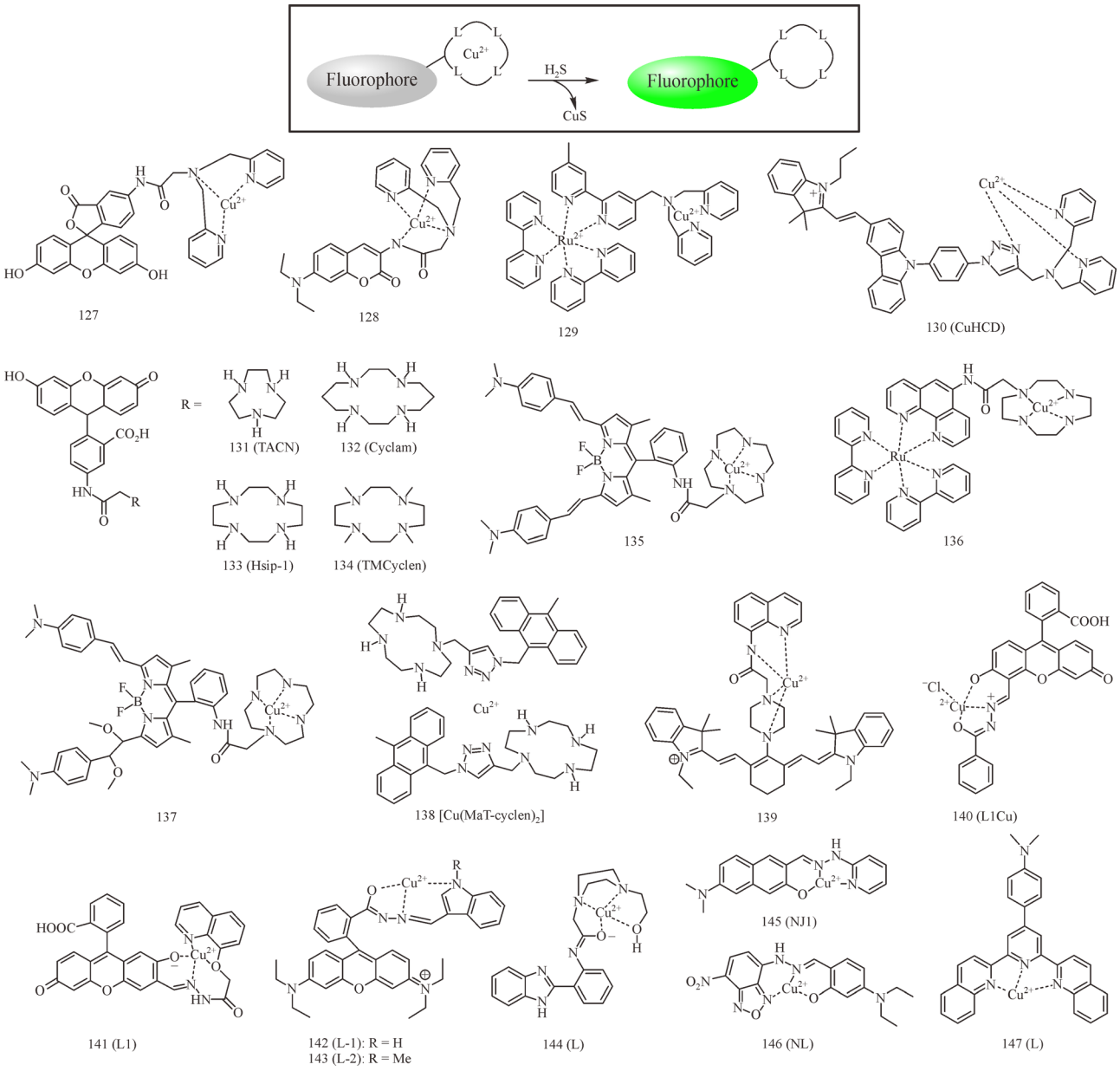

Fig. 10 Chemical structures of probes 127–147.

L (FITC-Ahx-Ser-Pro-Gly-His-NH_2) using fluorescein isothiocyanate as the fluorophore, Pro-Gly as the spacer, and histidine and serine as ionophores, which was designed and synthesized by solid phase peptide synthesis to chelate with Cu^{2+} to obtain the fluorescence chemosensor 152 (L-Cu) for H_2S detection [145]. In 2019, based on pyrene and benzothiozole hydrazide, Rajasekaran et al. reported a "on–off–on" fluorescence chemosensor. Despite the interference of other ions, the chemosensor had a high affinity for Cu^{2+} ions, and the 153 (DPD-Cu^{2+}) chelate still had a high sensitivity to S^{2-} ions through the displacement method [146].

Moreover, two-ligand and multi-ligand Cu(II) complex-based probes were developed. In 2013, Qu et al. developed a dipyrromethene-analogous NIR probe 154 (Cu-1) [147]. Later, in 2015, a BINOL-Benzimidazole-based probe 155 ($Cu(BB)_2$) was developed by Wang's group [148]. By applying the response of $Cu(BB)_2$ to H_2S, gaseous H_2S in air can be detected using a simple test strip. Another two-ligand Cu(II) complex-based probe 156 (AIE-S) was developed by our group [149]. The AIE-S-Cu complex ameliorates the poor water solubility of AIE-S, and the reaction product of H_2S and AIE-S will be fluorescent after rapid aggregation within seconds.

Other than taking Cu(II) complexation as a H_2S capturer, Kawagoe et al. obtained a Cd(II)-based probe 157 (6-CdII), after optimizing the coordination fragmentations and fluorophores [150]. Probe 157 (6-CdII) showed high stability against highly oxidative species (H_2O_2, HClO, $ONOO^-$, etc.) and had the best resistance towards GSH. Next, a mercury(II)-based probe 158 was developed by Wang's group [151]. By means of fluorescent indicating paper, probe 158 was capable of imaging H_2S gas even when coexisted with other gases, such as CO, NH_3, NO, NO_2, SO_2, etc. Chemical structures of probes 127–158 are shown in Figs. 10 and 11.

Compared with a variety of other probes for detecting biological H_2S, a key feature of metal sulfide-based probes is their prompt responses to H_2S with complete fluorescence within seconds. However, attributing to the existences of endogenous complex ions (including Zn^{2+} and Mg^{2+}), the proposed functions of designed probes may be abolished and the selectivity as well as the sensitivity would suffer from significant interference. In addition, the metabolism of the precipitate metal sulfides in human biology should be taken into consideration.

6 Fluorescent probes for H_2S_n

In recent studies, it was revealed that H_2S_n may play a practical mediator role in certain diseases related to H_2S. Therefore, the importance of H_2S_n in physiology and pathology is no less than that of H_2S. Although significant progress has been made in H_2S_n research in recent years, the distribution and regulatory mechanism of H_2S_n in the organism still need to be elucidated. Therefore, using fluorescence spectroscopy to analyze and explore the role of H_2S_n in a living system is a very effective method. At present, there are three types of probes for H_2S_n according to recognition units: 1) 2-fluoro-5-nitrobenzoic ester; 2) phenyl 2-(benzoylthio)benzoate; 3) H_2S_n mediated aziridine ring opening. In 2017, Gupta et al. had summarized the fluorescent probes for H_2S_n [152].

In 2014, Liu et al. developed the first H_2S_n-specific probes, employing a 2-fluoro-5-nitrobenzoic ester as H_2S_n recognition units [153]. The probes undergo nucleophilic aromatic substitution with H_2S_2 to form the intermediate persulfide, which promotes intramolecular cyclization to release the fluorophore. Although, 2-fluoro-5-nitrobenzoic esters can be consumed by biothiols, cyclization does not occur and thus affects the fluorescent signal of the probe.

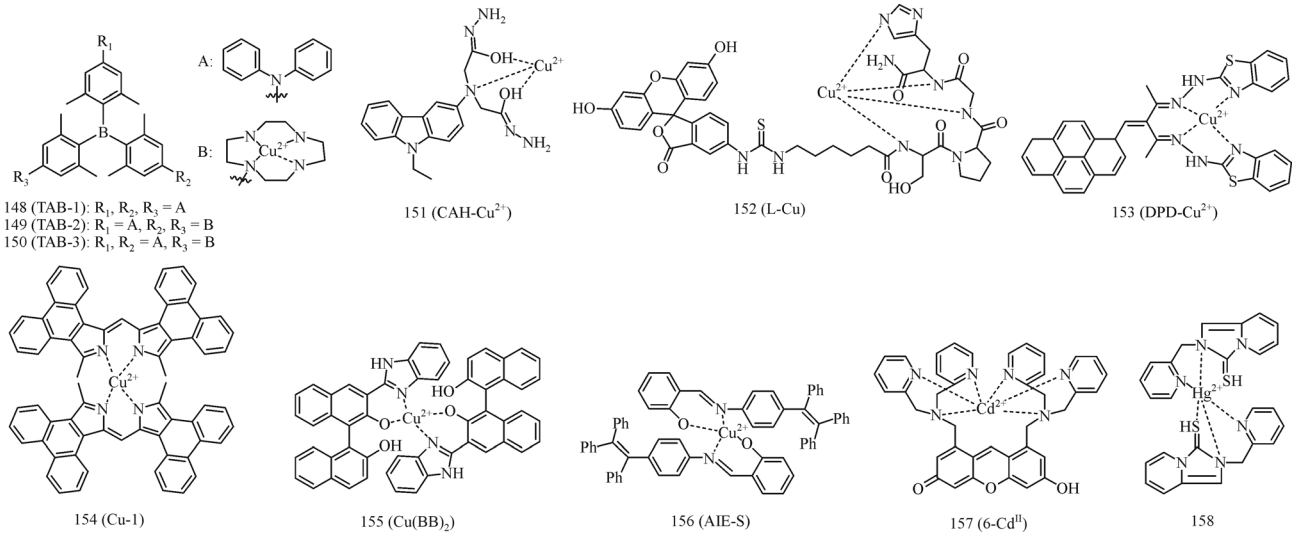

Fig. 11 Chemical structures of probes 148–158.

Subsequently, a large number of H_2S_n probes were developed, in which 2-fluoro-5-nitrobenzoic ester as H_2S_n recognition units was connected to different fluorophores skeleton. Reporters for H_2S_n based on semiheptamethine (159 (Cy-S_n)) [154], dicyanomethylene-benzopyran (160 (KB1)) [155], dicyanoisophorone (161 (RPHS1)) [156], phenothiazine (162–163 (PZC-S_n)) [157,158], resorufin (164 (Re-SS)) [159], BODIPY (165 (BDP-PHS)) [160], julolidine-coumarinocoumarins (166 (JCCF)) [161], naphthalene (167) [162] and so on have been described. Moreover, all those probes can be successfully applied in imaging of H_2S_n in living cells. In 2020, Zhao et al. reported a fluorescent probe 168 (MC-S_n) [163], which have two specific reaction sites for sulfide and can distinguish H_2S and H_2S_n according different fluorescence signals after reaction. It is helpful for us to study the interaction of H_2S and H_2S_n in biological systems. Besides, due to the superior performance of two-photon probe 168 (MC-S_n), it was applied to detect biothiols in liver tissues. In order to explore endogenous lysosome-targetable H_2S_n, Ren et al. developed a simple fluorescent probe 169 (NIPY-NF) [164]. In addition, utilizing morpholine group as the lysosomal targeting group, Han et al. designed probe 170 (Lyso-NRT-HP) for imaging of H_2S_n [165]. The results showed that probe 169 (NIPY-NF) and probe 170 (Lyso-NRT-HP) was effective for detecting endogenous H_2S_n, which produced in lysosome after lipopolysaccharides stimulates the cells. These probes are mainly used for imaging H_2S_n. None of probes can research H_2S_n formation via thionitrous acid (HSNO)-mediated. Zhang et al. developed an NIR fluorescent probe 171 (BCy-FN) for detection H_2S_n, which had used for observed the generation of H_2S_n in biological pathways for the first time [166]. The study reveals that this process was mediated by HSNO in living cells and *in vivo* under hypoxia stress. Chemical structures of probes 159–171 are shown in Fig. 12.

Utilizing the nucleophilicity and electrophilicity of H_2S_n, phenyl 2-(benzoylthio) benzoate unit is an excellent responsive group for H_2S_n. As depicted in Fig. 13, once the probe is in contact with H_2S_n, the benzothioester will react with H_2S_n to generate intermediate A; then H_2S_n keep to react with A to form intermediate B, which further cyclizes to release the fluorophore. In 2017, Fang et al. reported a NIR probe 172 based on the combination of a hemicyanine skeleton and phenyl 2-(benzoylthio) benzoate unit [167]. This probe can enable to capture H_2S_n effectively, which not only contribute to great sensitivity and selectivity, but also the potential functioning as living cells and mice imaging. Another probe 173 (τ-probe) was obtained to

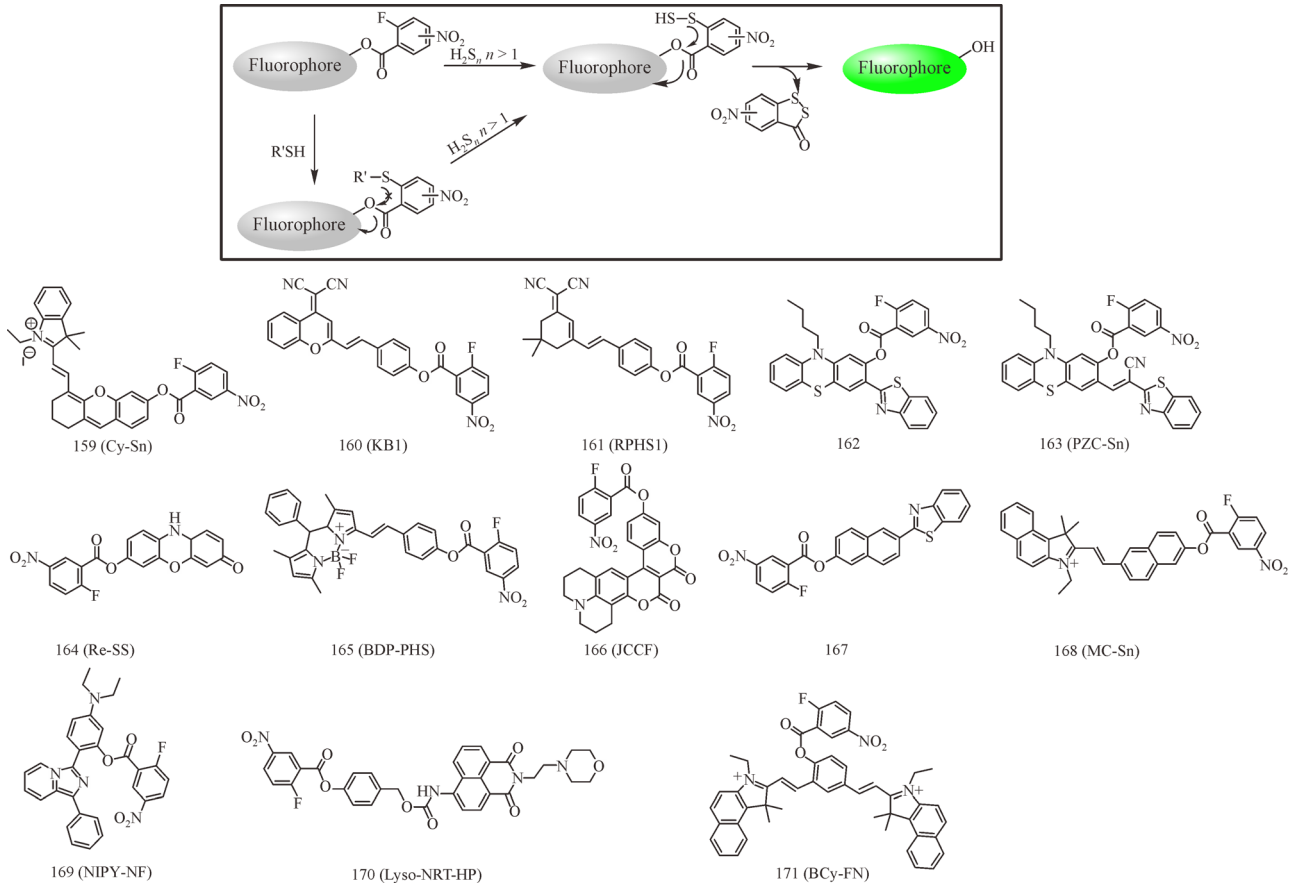

Fig. 12 Chemical structures of probes 159–171.

characterize H_2S_n by the changes of fluorescence lifetime rather than the change of fluorescence intensity by Yang et al., which can be widely utilized as an ultrasensitive implement for detecting H_2S_n in living systems [168]. Hoskere et al. designed a red-emitting probe 174 (MB-S_n) based on BODIPY scaffold, which performed conceivable amelioration of H_2S_n visualization in ER [169]. Coordinately, phenyl 2-(benzoylthio) benzoate group and heptamethine cyanine (HQO) are two main structures of probe 175 (HQO-PSP). This probe valid in mitochondrial H_2S_n sensing is versatile in tracking dynamic changes in living cells and tissues. Another two-photon fluorescent probe 176 (SPS-M1) was prepared by Kim'group [170]. Probe 176 (SPS-M1) was consisted of three functional parts: H_2S_n receptor part, fluorophore scaffold and mitochondria-targeting unit, which was explored for distinguishing mitochondrial H_2S_n in living cells with high sensitivity and selectivity. In 2020, Liang et al. reported probe 177 (PP-PS) for imaging endogenous H_2S_n lysosomal localization, which can apply to further visualize endogenous H_2S_n in the animal inflammation model [171]. Chemical structures of probes 172–177 are shown in Fig. 13.

In recent years, people have paid more attention to H_2S_n, various probes emerge in endlessly. On the sensitivity and selectivity of the probes already have a lot of immense progress. However, combined current optical imaging technology, if the probe of H_2S_n needs further development, its background fluorescence, toxicity and stability of the probe in complex systems should be worthy of consideration.

7 Conclusions

In the last decade, significant efforts have been made to develop fluorescent probes for detecting H_2S. Various engineering strategies have been utilized to optimize the optical properties as well as the biological compatibility. Reduction-based, nucleophilicity-based, and metal sulfide-based strategies are the most widely applied strategies. According to these strategies, a considerable number of probes were gained, some of which have already been utilized to image H_2S in cells, tissues, even within the living organism. At the same time, the advancement of modern imaging apparatuses also allows for distinct and high-quality detection for the low concentration of H_2S in organisms. Moreover, due to the significant of H_2S_n in physiology and pathology, we also introduced some probes for H_2S_n. We believe that this review will enable more researchers to understand the design strategies of H_2S and H_2S_n, and lead to further research in this field.

The goal of small-molecular chemical probes for benignant is to realize in real-time, precise and convenient detection of the limited concentration of H_2S and H_2S_n *in vivo*, which will allow for the development of further applications upon this crucial biological matter. Also, the advances of H_2S and H_2S_n chemical probes will be beneficial to reveal the complexity and intricacy of its biological processes. However, there is still a gap between the current research status and practical applications. Except for improving the selectivity and sensitivity of probes, the biological compatibility and biological stability

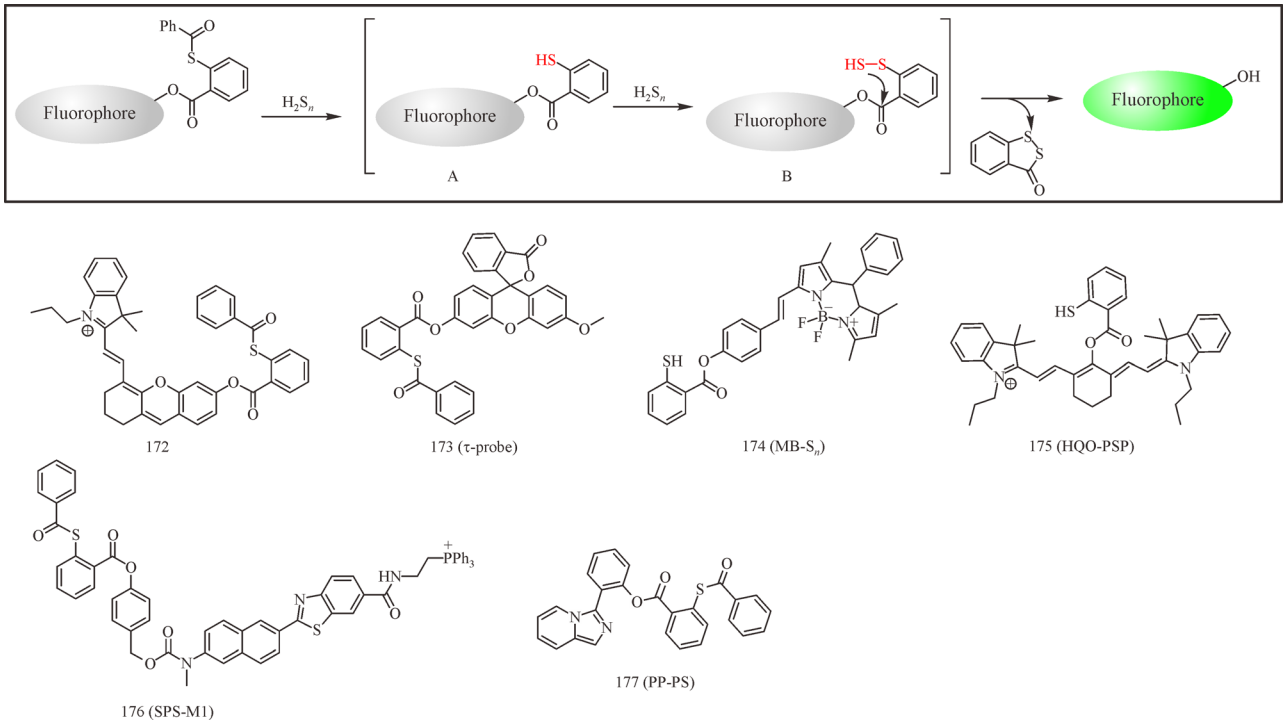

Fig. 13 Chemical structures of probes 172–177.

should also be taken into consideration. Although, in recent years, the research on H_2S probes has slowed down, after we understand the complex pathological and physiological functions of H_2S and H_2S_n, the ultimate goal of our continuing research will be to achieve disease treatment. The future decade is going to witness an exciting and tremendous leap of fluorescent probes for H_2S and H_2S_n.

Acknowledgements This work was supported by China Postdoctoral Science Foundation (Grant No. 2019M652053).

References

1. Barr L A, Calvert J W. Discoveries of hydrogen sulfide as a novel cardiovascular therapeutic. Circulation Journal, 2014, 78(9): 2111–2118
2. Brancaleone V, Mitidieri E, Flower R J, Cirino G, Perretti M. Annexin A1 mediates hydrogen sulfide properties in the control of inflammation. Journal of Pharmacology and Experimental Therapeutics, 2014, 351(1): 96–104
3. Chen W L, Niu Y Y, Jiang W Z, Tang H L, Zhang C, Xia Q M, Tang X Q. Neuroprotective effects of hydrogen sulfide and the underlying signaling pathways. Reviews in the Neurosciences, 2015, 26(2): 129–142
4. Hosoki R, Matsuki N, Kimura H. The possible role of hydrogen sulfide as an endogenous smooth muscle relaxant in synergy with nitric oxide. Biochemical and Biophysical Research Communications, 1997, 237(3): 527–531
5. Abdelrahman R S, El-Awady M S, Nader M A, Ammar E M. Hydrogen sulfide ameliorates cardiovascular dysfunction induced by cecal ligation and puncture in rats. Human and Experimental Toxicology, 2015, 34(10): 953–964
6. Cheung S H, Kwok W K, To K F, Lau J Y. Anti-atherogenic effect of hydrogen sulfide by over-expression of cystathionine γ-lyase (CSE) gene. PLoS One, 2014, 9(11): e113038
7. Liu Z, Han Y, Li L, Lu H, Meng G, Li X, Shirhan M, Peh M T, Xie L, Zhou S, et al. The hydrogen sulfide donor, GYY4137, exhibits anti-atherosclerotic activity in high fat fed apolipoprotein E(-/-) mice. British Journal of Pharmacology, 2013, 169(8): 1795–1809
8. Jain S K, Huning L, Micinski D. Hydrogen sulfide upregulates glutamate-cysteine ligase catalytic subunit, glutamate-cysteine ligase modifier subunit, and glutathione and inhibits interleukin-1beta secretion in monocytes exposed to high glucose levels. Metabolic Syndrome and Related Disorders, 2014, 12(5): 299–302
9. Sieghart D, Liszt M, Wanivenhaus A, Broll H, Kiener H, Klosch B, Steiner G. Hydrogen sulphide decreases IL-1β-induced activation of fibroblast-like synoviocytes from patients with osteoarthritis. Journal of Cellular and Molecular Medicine, 2015, 19(1): 187–197
10. Giuliani D, Ottani A, Zaffe D, Galantucci M, Strinati F, Lodi R, Guarini S. Hydrogen sulfide slows down progression of experimental Alzheimer's disease by targeting multiple pathophysiological mechanisms. Neurobiology of Learning and Memory, 2013, 104: 82–91
11. Wang M, Zhu J, Pan Y, Dong J, Zhang L, Zhang X, Zhang L. Hydrogen sulfide functions as a neuromodulator to regulate striatal neurotransmission in a mouse model of Parkinson's disease. Journal of Neuroscience Research, 2015, 93(3): 487–494
12. Magierowski M, Jasnos K, Kwiecien S, Drozdowicz D, Surmiak M, Strzalka M, Ptak B A, Wallace J L, Brzozowski T. Endogenous prostaglandins and afferent sensory nerves in gastroprotective effect of hydrogen sulfide against stress-induced gastric lesions. PLoS One, 2015, 10(3): e0118972
13. DeRatt B N, Ralat M A, Kabil O, Chi Y Y, Banerjee R, Gregory J F III. Vitamin B-6 restriction reduces the production of hydrogen sulfide and its biomarkers by the transsulfuration pathway in cultured human hepatoma cells. Journal of Nutrition, 2014, 144 (10): 1501–1508
14. Kimura H. Production and physiological effects of hydrogen sulfide. Antioxidants & Redox Signaling, 2014, 20(5): 783–793
15. Whiteman M, Moore P K. Hydrogen sulfide and the vasculature: a novel vasculoprotective entity and regulator of nitric oxide bioavailability? Journal of Cellular and Molecular Medicine, 2009, 13(3): 488–507
16. Lin V S, Chang C J. Fluorescent probes for sensing and imaging biological hydrogen sulfide. Current Opinion in Chemical Biology, 2012, 16(5-6): 595–601
17. Yu F, Han X, Chen L. Fluorescent probes for hydrogen sulfide detection and bioimaging. Chemical Communications, 2014, 50 (82): 12234–12249
18. Guo Z, Chen G, Zeng G, Li Z, Chen A, Wang J, Jiang L. Fluorescence chemosensors for hydrogen sulfide detection in biological systems. Analyst (London), 2015, 140(6): 1772–1786
19. Lin V S, Chen W, Xian M, Chang C J. Chemical probes for molecular imaging and detection of hydrogen sulfide and reactive sulfur species in biological systems. Chemical Society Reviews, 2015, 44(14): 4596–4618
20. Yi L, Xi Z. Thiolysis of NBD-based dyes for colorimetric and fluorescence detection of H_2S and biothiols: design and biological applications. Organic & Biomolecular Chemistry, 2017, 15(18): 3828–3839
21. Lippert A R, New E J, Chang C J. Reaction-based fluorescent probes for selective imaging of hydrogen sulfide in living cells. Journal of the American Chemical Society, 2011, 133(26): 10078–10080
22. Chen W, Pacheco A, Takano Y, Day J J, Hanaoka K, Xian M. A single fluorescent probe to visualize hydrogen sulfide and hydrogen polysulfides with different fluorescence signals. Angewandte Chemie International Edition, 2016, 128(34): 10147–10150
23. Zhao Q, Huo F, Kang J, Zhang Y, Yin C. A novel FRET-based fluorescent probe for the selective detection of hydrogen sulfide (H_2S) and its application for bioimaging. Journal of Materials Chemistry. B, Materials for Biology and Medicine, 2018, 6(30): 4903–4908
24. Jiao X, Xiao Y, Li Y, Liang M, Xie X, Wang X, Tang B. Evaluating drug-induced liver injury and its remission via discrimination and imaging of HClO and H_2S with a two-photon fluorescent probe. Analytical Chemistry, 2018, 90(12): 7510–7516
25. Ren M, Li Z, Deng B, Wang L, Lin W. Single fluorescent probe separately and continuously visualize H_2S and HClO in lysosomes

with different fluorescence signals. Analytical Chemistry, 2019, 91 (4): 2932–2938
26. Wu Z, Liang D, Tang X. Visualizing hydrogen sulfide in mitochondria and lysosome of living cells and in tumors of living mice with positively charged fluorescent chemosensors. Analytical Chemistry, 2016, 88(18): 9213–9218
27. Deng B, Ren M, Wang J Y, Zhou K, Lin W. A mitochondrial-targeted two-photon fluorescent probe for imaging hydrogen sulfide in the living cells and mouse liver tissues. Sensors and Actuators. B, Chemical, 2017, 248: 50–56
28. Tang Y, Xu A, Ma Y, Xu G, Gao S, Lin W. A turn-on endoplasmic reticulum-targeted two-photon fluorescent probe for hydrogen sulfide and bio-imaging applications in living cells, tissues, and zebrafish. Scientific Reports, 2017, 7(1): 1–9
29. Fu Y J, Yao H W, Zhu X Y, Guo X F, Wang H. A cell surface specific two-photon fluorescent probe for monitoring intercellular transmission of hydrogen sulfide. Analytica Chimica Acta, 2017, 994: 1–9
30. Song X, Dong B, Kong X, Wang C, Zhang N, Lin W. A cancer cell-specific two-photon fluorescent probe for imaging hydrogen sulfide in living cells. RSC Advances, 2017, 7(26): 15817–15822
31. Chen J, Zhao M, Jiang X, Sizovs A, Wang M C, Provost C R, Huang J, Wang J. Genetically anchored fluorescent probes for subcellular specific imaging of hydrogen sulfide. Analyst (London), 2016, 141(4): 1209–1213
32. Zhu Z, Li Y, Wei C, Wen X, Xi Z, Yi L. Multi-fluorinated azido coumarins for rapid and selective detection of biological H_2S in living cells. Chemistry, an Asian Journal, 2016, 11(1): 68–71
33. Velusamy N, Binoy A, Bobba K N, Nedungadi D, Mishra N, Bhuniya S. A bioorthogonal fluorescent probe for mitochondrial hydrogen sulfide: new strategy for cancer cell labeling. Chemical Communications, 2017, 53(62): 8802–8805
34. Xie Q L, Liu W, Liu X J, Ouyang F, Kuang Y Q, Jiang J H. An azidocoumarin-based fluorescent probe for imaging lysosomal hydrogen sulfide in living cells. Analytical Methods, 2017, 9(19): 2859–2864
35. Liu K, Liu C, Shang H, Ren M, Lin W. A novel red light emissive two-photon fluorescent probe for hydrogen sulfide (H_2S) in nucleolus region and its application for H_2S detection in zebrafish and live mice. Sensors and Actuators. B, Chemical, 2018, 256: 342–350
36. Qiao Z, Zhang H, Wang K, Zhang Y. A highly sensitive and responsive fluorescent probe based on 6-azide-chroman dye for detection and imaging of hydrogen sulfide in cells. Talanta, 2019, 195: 850–856
37. Dai C G, Liu X L, Du X J, Zhang Y, Song Q H. Two-input fluorescent probe for thiols and hydrogen sulfide chemosensing and live cell imaging. ACS Sensors, 2016, 1(7): 888–895
38. Ren T B, Xu W, Zhang Q L, Zhang X X, Wen S Y, Yi H B, Yuan L, Zhang X B. Enhancing the anti-solvatochromic two-photon fluorescence for cirrhosis imaging by forming a hydrogen-bond network. Angewandte Chemie International Edition, 2018, 57(25): 7473–7477
39. Dou Y, Gu X, Ying S, Zhu S, Yu S, Shen W, Zhu Q. A novel lysosome-targeted fluorogenic probe based on 5-triazole-quinoline for the rapid detection of hydrogen sulfide in living cells. Organic & Biomolecular Chemistry, 2018, 16(5): 712–716
40. Shen D, Liu J, Sheng L, Lv Y, Wu G, Wang P, Du K. Design, synthesis and evaluation of a novel fluorescent probe to accurately detect H_2S in hepatocytes and natural waters. Spectrochimica Acta. Part A: Molecular and Biomolecular Spectroscopy, 2020, 228: 117690
41. Zhu H, Liang C, Cai X, Zhang H, Liu C, Jia P, Li Z, Yu Y, Zhang X, Sheng W, Zhu B. Rational design of a targetable fluorescent probe for visualizing H_2S production under Golgi stress response elicited by monensin. Analytical Chemistry, 2020, 92(2): 1883–1889
42. Bailey T S, Pluth M D. Chemiluminescent detection of enzymatically produced hydrogen sulfide: substrate hydrogen bonding influences selectivity for H_2S over biological thiols. Journal of the American Chemical Society, 2013, 135(44): 16697–16704
43. Wang L, Chen X, Cao D. A nitroolefin functionalized DPP fluorescent probe for the selective detection of hydrogen sulfide. New Journal of Chemistry, 2017, 41(9): 3367–3373
44. Zhou N, Yin C, Chao J, Zhang Y, Huo F. An isoxazole-accelerated nitro oxidation type fluorescent detection and imaging for hydrogen sulfide in cells. Sensors and Actuators. B, Chemical, 2019, 287: 131–137
45. Li X, Cheng J, Gong Y, Yang B, Hu Y. Mapping hydrogen sulfide in rats with a novel azo-based fluorescent probe. Biosensors & Bioelectronics, 2015, 65: 302–306
46. Chen B, Huang J, Geng H, Xuan L, Xu T, Li X, Han Y. A new ESIPT-based fluorescent probe for highly selective and sensitive detection of hydrogen sulfide and its application in live-cell imaging. New Journal of Chemistry, 2017, 41(3): 1119–1123
47. Lippert A R. Designing reaction-based fluorescent probes for selective hydrogen sulfide detection. Journal of Inorganic Biochemistry, 2014, 133: 136–142
48. Montoya L A, Pearce T F, Hansen R J, Zakharov L N, Pluth M D. Development of selective colorimetric probes for hydrogen sulfide based on nucleophilic aromatic substitution. Journal of Organic Chemistry, 2013, 78(13): 6550–6557
49. Wu X, Shi J, Yang L, Han J, Han S. A near-infrared fluorescence dye for sensitive detection of hydrogen sulfide in serum. Bioorganic & Medicinal Chemistry Letters, 2014, 24(1): 314–316
50. Li X, Tang Y, Li J, Hu X, Yin C, Yang Z, Wang Q, Wu Z, Lu X, Wang W, Huang W, Fan Q. A small-molecule probe for ratiometric photoacoustic imaging of hydrogen sulfide in living mice. Chemical Communications, 2019, 55(42): 5934–5937
51. Ren M, Deng B, Kong X, Zhou K, Liu K, Xu G, Lin W. A TICT-based fluorescent probe for rapid and specific detection of hydrogen sulfide and its bio-imaging applications. Chemical Communications, 2016, 52(38): 6415–6418
52. Feng X, Zhang T, Liu J T, Miao J Y, Zhao B X. A new ratiometric fluorescent probe for rapid, sensitive and selective detection of endogenous hydrogen sulfide in mitochondria. Chemical Communications, 2016, 52(15): 3131–3134
53. Liu Y, Meng F, He L, Liu K, Lin W. A dual-site two-photon fluorescent probe for visualizing lysosomes and tracking lysosomal hydrogen sulfide with two different sets of fluorescence signals in the living cells and mouse liver tissues. Chemical Communica-

tions, 2016, 52(43): 7016–7019
54. He L, Yang X, Liu Y, Weiying Lin W L. Colorimetric and ratiometric fluorescent probe for hydrogen sulfide using a coumarin-pyronine FRET dyad with a large emission shift. Analytical Methods, 2016, 8(45): 8022–8027
55. Li Y, Gu B, Su W, Duan X, Xu H, Huang Z, Li H, Yao S. A simple and efficient fluorescent probe for the rapid detection of H_2S in living cells and on agar gels. Analytical Methods, 2017, 9(22): 3290–3295
56. Ma J, Li F, Li Q, Li Y, Yan C, Lu X, Guo Y. Naked-eye and ratiometric fluorescence probe for fast and sensitive detection of hydrogen sulfide and its application in bioimaging. New Journal of Chemistry, 2018, 42(23): 19272–19278
57. Ma Y, Wang H, Su S, Chen Y, Li Y, Wang X, Wang Z. A red mitochondria-targeted AIEgen for visualizing H_2S in living cells and tumours. Analyst (London), 2019, 144(10): 3381–3388
58. Liu Y, Niu J, Wang W, Ma Y, Lin W. Simultaneous imaging of ribonucleic acid and hydrogen sulfide in living systems with distinct fluorescence signals using a single fluorescent probe. Advancement of Science, 2018, 5(7): 1700966
59. Cui J, Zhang T, Sun Y Q, Li D P, Liu J T, Zhao B X. A highly sensitive and selective fluorescent probe for H_2S detection with large fluorescence enhancement. Sensors and Actuators. B, Chemical, 2016, 232: 705–711
60. Zhang L, Zheng X E, Zou F, Shang Y, Meng W, Lai E, Xu Z, Liu Y, Zhao J. A highly selective and sensitive near-infrared fluorescent probe for imaging of hydrogen sulphide in living cells and mice. Scientific Reports, 2016, 6(1): 18868
61. Zhang P, Nie X, Gao M, Zeng F, Qin A, Wu S, Tang B Z. A highly selective fluorescent nanoprobe based on AIE and ESIPT for imaging hydrogen sulfide in live cells and zebrafish. Materials Chemistry Frontiers, 2017, 1(5): 838–845
62. Zhou L, Lu D, Wang Q, Liu S, Lin Q, Sun H. Molecular engineering of a mitochondrial-targeting two-photon in and near-infrared out fluorescent probe for gaseous signal molecules H_2S in deep tissue bioimaging. Biosensors & Bioelectronics, 2017, 91: 699–705
63. Gu B, Su W, Huang L, Wu C, Duan X, Li Y, Xu H, Huang Z, Li H, Yao S. Real-time tracking and selective visualization of exogenous and endogenous hydrogen sulfide by a near-infrared fluorescent probe. Sensors and Actuators. B, Chemical, 2018, 255: 2347–2355
64. Qian M, Zhang L, Pu Z, Xia J, Chen L, Xia Y, Cui H, Wang J, Peng X. A NIR fluorescent probe for the detection and visualization of hydrogen sulfide using the aldehyde group assisted thiolysis of dinitrophenyl ether strategy. Journal of Materials Chemistry. B, Materials for Biology and Medicine, 2018, 6(47): 7916–7925
65. Chen S, Li H, Hou P. A novel imidazo[1,5-α]pyridine-based fluorescent probe with a large Stokes shift for imaging hydrogen sulfide. Sensors and Actuators. B, Chemical, 2018, 256: 1086–1092
66. Ji Y, Xia L J, Chen L, Guo X F, Wang H, Zhang H J. A novel BODIPY-based fluorescent probe for selective detection of hydrogen sulfide in living cells and tissues. Talanta, 2018, 181: 104–111
67. Li Y T, Zhao X J, Jiang Y R, Yang B Q. A novel long-wavelength fluorescent probe for selective detection of hydrogen sulfide in living cells. New Journal of Chemistry, 2018, 42(24): 19478–19484
68. Liu J, Chen X, Zhang Y, Gao G, Zhang X, Hou S, Hou Y. A novel 3-hydroxychromone fluorescent probe for hydrogen sulfide based on an excited-state intramolecular proton transfer mechanism. New Journal of Chemistry, 2018, 42(15): 12918–12923
69. Wu C, Hu X, Gu B, Yin P, Su W, Li Y, Lu Q, Zhang Y, Li H. A lysosome-targeting colorimetric and fluorescent dual signal probe for sensitive detection and bioimaging of hydrogen sulfide. Analytical Methods, 2018, 10(6): 604–610
70. Yang L, Zhao J, Yu X, Zhang R, Han G, Liu R, Liu Z, Zhao T, Han M Y, Zhang Z. Dynamic mapping of spontaneously produced H_2S in the entire cell space and in live animals using a rationally designed molecular switch. Analyst (London), 2018, 143(8): 1881–1889
71. Sun L, Wu Y, Chen J, Zhong J, Zeng F, Wu S. A turn-on optoacoustic probe for imaging metformin-induced upregulation of hepatic hydrogen sulfide and subsequent liver injury. Theranostics, 2019, 9(1): 77–89
72. Zhao X J, Li Y T, Jiang Y R, Yang B Q, Liu C, Liu Z H. A novel "turn-on" mitochondria-targeting near-infrared fluorescent probe for H_2S detection and in living cells imaging. Talanta, 2019, 197: 326–333
73. Zhu X Y, Wu H, Guo X F, Wang H. Novel BODIPY-based fluorescent probes with large stokes shift for imaging hydrogen sulfide. Dyes and Pigments, 2019, 165: 400–407
74. Fang T, Jiang X D, Sun C, Li Q. BODIPY-based naked-eye fluorescent on-off probe with high selectivity for H_2S based on thiolysis of dinitrophenyl ether. Sensors and Actuators. B, Chemical, 2019, 290: 551–557
75. Su D, Cheng D, Lv Y, Ren X, Wu Q, Yuan L. A unique off-on near-infrared QCy7-derived probe for selective detection and imaging of hydrogen sulfide in cells and *in vivo*. Spectrochimica Acta. Part A: Molecular and Biomolecular Spectroscopy, 2020, 226: 117635
76. Lin X, Lu X, Zhou J, Ren H, Dong X, Zhao W, Chen Z. Instantaneous fluorescent probe for the specific detection of H_2S. Spectrochimica Acta. Part A: Molecular and Biomolecular Spectroscopy, 2019, 213: 416–422
77. Zhang Y, Zhang B, Li Z, Wang L, Ren X, Ye Y. Endoplasmic reticulum targeted fluorescent probe for the detection of hydrogen sulfide based on a twist-blockage strategy. Organic & Biomolecular Chemistry, 2019, 17(38): 8778–8783
78. Zhong K, Zhou S, Yan X, Li X, Hou S, Cheng L, Gao X, Li Y, Tang L. A simple H_2S fluorescent probe with long wavelength emission: application in water, wine, living cells and detection of H_2S gas. Dyes and Pigments, 2020, 174: 108049
79. Ding S, Feng G. Smart probe for rapid and simultaneous detection and discrimination of hydrogen sulfide, cysteine/homocysteine, and glutathione. Sensors and Actuators. B, Chemical, 2016, 235: 691–697
80. Ding S, Feng W, Feng G. Rapid and highly selective detection of H_2S by nitrobenzofurazan (NBD) ether-based fluorescent probes with an aldehyde group. Sensors and Actuators. B, Chemical, 2017, 238: 619–625
81. Wang R, Li Z, Zhang C, Li Y, Xu G, Zhang Q Z, Li L Y, Yi L, Xi

Z. Fast-response turn-on fluorescent probes based on thiolysis of NBD amine for H_2S bioimaging. ChemBioChem, 2016, 17(10): 962–968

82. Grimm J B, English B P, Chen J, Slaughter J P, Zhang Z, Revyakin A, Patel R, Macklin J J, Normanno D, Singer R H, et al. A general method to improve fluorophores for live-cell and single-molecule microscopy. Nature Methods, 2015, 12(3): 244–250
83. Ismail I, Wang D, Wang D, Niu C, Huang H, Yi L, Xi Z. A mitochondria-targeted red-emitting probe for imaging hydrogen sulfide in living cells and zebrafish. Organic & Biomolecular Chemistry, 2019, 17(13): 3389–3395
84. Wei C, Wei L, Xi Z, Yi L. A FRET-based fluorescent probe for imaging H_2S in living cells. Tetrahedron Letters, 2013, 54(50): 6937–6939
85. Ismail I, Wang D, Wang Z, Wang D, Zhang C, Yi L, Xi Z. A julolidine-fused coumarin-NBD dyad for highly selective and sensitive detection of H_2S in biological samples. Dyes and Pigments, 2019, 163: 700–706
86. Huang Y, Zhang C, Xi Z, Yi L. Synthesis and characterizations of a highly sensitive and selective fluorescent probe for hydrogen sulfide. Tetrahedron Letters, 2016, 57(10): 1187–1191
87. Zhang H, Chen J, Xiong H, Zhang Y, Chen W, Sheng J, Song X. An endoplasmic reticulum-targetable fluorescent probe for highly selective detection of hydrogen sulfide. Organic & Biomolecular Chemistry, 2019, 17(6): 1436–1441
88. Pak Y L, Li J, Ko K C, Kim G, Lee J Y, Yoon J. Mitochondria-targeted reaction-based fluorescent probe for hydrogen sulfide. Analytical Chemistry, 2016, 88(10): 5476–5481
89. Hou P, Li H, Chen S. A highly selective and sensitive 3-hydroxyflavone-based colorimetric and fluorescent probe for hydrogen sulfide with a large Stokes shift. Tetrahedron, 2016, 72 (24): 3531–3534
90. Kang J, Huo F, Ning P, Meng X, Chao J, Yin C. Two red-emission single and double 'arms' fluorescent materials stemed from 'one-pot' reaction for hydrogen sulfide vivo imaging. Sensors and Actuators. B, Chemical, 2017, 250: 342–350
91. Zhang J, Ji X, Zhou J, Chen Z, Dong X, Zhao W. Pyridinium substituted BODIPY as NIR fluorescent probe for simultaneous sensing of hydrogen sulphide/glutathione and cysteine/homocysteine. Sensors and Actuators. B, Chemical, 2018, 257: 1076–1082
92. Wang Y, Lv X, Guo W. A reaction-based and highly selective fluorescent probe for hydrogen sulfide. Dyes and Pigments, 2017, 139: 482–486
93. Xiong J, Xia L, Huang Q, Huang J, Gu Y, Wang P. Cyanine-based NIR fluorescent probe for monitoring H_2S and imaging in living cells and *in vivo*. Talanta, 2018, 184: 109–114
94. Tang Y, Jiang G F. A novel two-photon fluorescent probe for hydrogen sulfide in living cells using an acedan-NBD amine dyad based on FRET process with high selectivity and sensitivity. New Journal of Chemistry, 2017, 41(14): 6769–6774
95. Cui L, Zhong Y, Zhu W, Xu Y, Du Q, Wang X, Qian X, Xiao Y. A new prodrug-derived ratiometric fluorescent probe for hypoxia: high selectivity of nitroreductase and imaging in tumor cell. Organic Letters, 2011, 13(5): 928–931
96. Zhang L, Meng W Q, Lu L, Xue Y S, Li C, Zou F, Liu Y, Zhao J. Selective detection of endogenous H_2S in living cells and the mouse hippocampus using a ratiometric fluorescent probe. Scientific Reports, 2015, 4(1): 5870
97. Zhang H, Xie Y, Wang P, Chen G, Liu R, Lam Y W, Hu Y, Zhu Q, Sun H. An iminocoumarin benzothiazole-based fluorescent probe for imaging hydrogen sulfide in living cells. Talanta, 2015, 135: 149–154
98. Wang J, Chen Y, Yang C, Wei T, Han Y, Xia M. An ICT-based colorimetric and ratiometric fluorescent probe for hydrogen sulfide and its application in live cell imaging. RSC Advances, 2016, 6 (39): 33031–33035
99. Steiger A K, Pardue S, Kevil C G, Pluth M D. Self-Immolative thiocarbamates provide access to triggered H_2S donors and analyte replacement fluorescent probes. Journal of the American Chemical Society, 2016, 138(23): 7256–7259
100. Feng W, Mao Z, Liu L, Liu Z. A ratiometric two-photon fluorescent probe for imaging hydrogen sulfide in lysosomes. Talanta, 2017, 167: 134–142
101. Thirumalaivasan N, Venkatesan P, Wu S P. Highly selective turn-on probe for H_2S with imaging applications *in vitro* and *in vivo*. New Journal of Chemistry, 2017, 41(22): 13510–13515
102. Park C S, Ha T H, Choi S A, Nguyen D N, Noh S, Kwon O S, Lee C S, Yoon H. A near-infrared "turn-on" fluorescent probe with a self-immolative linker for the *in vivo* quantitative detection and imaging of hydrogen sulfide. Biosensors & Bioelectronics, 2017, 89: 919–926
103. Li S J, Li Y F, Liu H W, Zhou D Y, Jiang W L, Ou Yang J, Li C Y. A dual-response fluorescent probe for the detection of viscosity and H_2S and its application in studying their cross-talk influence in mitochondria. Analytical Chemistry, 2018, 90(15): 9418–9425
104. Zhao Q, Yin C, Kang J, Wen Y, Huo F. A viscosity sensitive azide-pyridine BODIPY-based fluorescent dye for imaging of hydrogen sulfide in living cells. Dyes and Pigments, 2018, 159: 166–172
105. Zhou T, Yang Y, Zhou K, Jin M, Han M, Li W, Yin C. Efficiently mitochondrial targeting fluorescent imaging of H_2S *in vivo* based on a conjugate-lengthened cyanine NIR fluorescent probe. Sensors and Actuators. B, Chemical, 2019, 301: 127116
106. Yang L, Su Y, Sha Z, Geng Y, Qi F, Song X. A red-emitting fluorescent probe for hydrogen sulfide in living cells with a large stokes shift. Organic & Biomolecular Chemistry, 2018, 16(7): 1150–1156
107. Zhu L, Liao W, Chang H, Liu X, Miao S. A novel fluorescent probe for detection of hydrogen sulfide and its bioimaging applications in living cells. ChemistrySelect, 2020, 5(2): 829–833
108. Li D P, Zhang J F, Cui J, Ma X F, Liu J T, Miao J Y, Zhao B X. A ratiometric fluorescent probe for fast detection of hydrogen sulfide and recognition of biological thiols. Sensors and Actuators. B, Chemical, 2016, 234: 231–238
109. Kang J, Huo F, Yin C. A novel ratiometric fluorescent H_2S probe based on tandem nucleophilic substitution/cyclization reaction and its bioimaging. Dyes and Pigments, 2017, 146: 287–292
110. Men J, Yang X, Zhang H, Zhou J. A near-infrared fluorescent probe based on nucleophilic substitution-cyclization for selective detection of hydrogen sulfide and bioimaging. Dyes and Pigments, 2018, 153: 206–212
111. Zhang X, Sun R, Duan G, Zhou Z, Luo Y, Li W, Zhang L, Gu Y, Zha X. A highly sensitive near-infrared fluorescent probe for the

detection of hydrogen sulfide and its application in living cells and mice. New Journal of Chemistry, 2018, 42(24): 19795–19800

112. Cao T, Teng Z, Gong D, Qian J, Liu W, Iqbal K, Qin W, Guo H. A ratiometric fluorescent probe for detection of endogenous and exogenous hydrogen sulfide in living cells. Talanta, 2019, 198: 185–192
113. Wang H, Yang D, Tan R, Zhou Z J, Xu R, Zhang J F, Zhou Y. A cyanine-based colorimetric and fluorescence probe for detection of hydrogen sulfide *in vivo*. Sensors and Actuators. B, Chemical, 2017, 247: 883–888
114. Wang J, Wen Y, Huo F, Yin C. A highly sensitive fluorescent probe for hydrogen sulfide based on dicyanoisophorone and its imaging in living cells. Sensors and Actuators. B, Chemical, 2019, 294: 141–147
115. Guan H, Zhang A, Li P, Xia L, Guo F. ESIPT fluorescence probe based on double-switch recognition mechanism for selective and rapid detection of hydrogen sulfide in living cells. ACS Omega, 2019, 4(5): 9113–9119
116. Qian Y, Karpus J, Kabil O, Zhang S Y, Zhu H L, Banerjee R, Zhao J, He C. Selective fluorescent probes for live-cell monitoring of sulphide. Nature Communications, 2011, 2(1): 495
117. Li X, Zhang S, Cao J, Xie N, Liu T, Yang B, He Q, Hu Y. An ICT-based fluorescent switch-on probe for hydrogen sulfide in living cells. Chemical Communications, 2013, 49(77): 8656–8658
118. Singha S, Kim D, Moon H, Wang T, Kim K H, Shin Y H, Jung J, Seo E, Lee S J, Ahn K H. Toward a selective, sensitive, fast-responsive, and biocompatible two-photon probe for hydrogen sulfide in live cells. Analytical Chemistry, 2015, 87(2): 1188–1195
119. Ryu H G, Singha S, Jun Y W, Reo Y J, Ahn K H. Two-photon fluorescent probe for hydrogen sulfide based on a red-emitting benzocoumarin dye. Tetrahedron Letters, 2018, 59(1): 49–53
120. Chen X, Wu S, Han J, Han S. Rhodamine-propargylic esters for detection of mitochondrial hydrogen sulfide in living cells. Bioorganic & Medicinal Chemistry Letters, 2013, 23(19): 5295–5299
121. Sathyadevi P, Chen Y J, Wu S C, Chen Y H, Wang Y M. Reaction-based epoxide fluorescent probe for *in vivo* visualization of hydrogen sulfide. Biosensors & Bioelectronics, 2015, 68: 681–687
122. Karakus E, Ucuncu M, Emrullahoglu M. Electrophilic cyanate as a recognition motif for reactive sulfur species: selective fluorescence detection of H_2S. Analytical Chemistry, 2016, 88(1): 1039–1043
123. Xu G, Yan Q, Lv X, Zhu Y, Xin K, Shi B, Wang R, Chen J, Gao W, Shi P, Fan C, Zhao C, Tian H. Imaging of colorectal cancers using activatable nanoprobes with second near-infrared window emission. Angewandte Chemie International Edition, 2018, 57(14): 3626–3630
124. Zhao Z, Cao L, Zhang T, Hu R, Wang S, Li S, Li Y, Yang G. Novel reaction-based fluorescence probes for the detection of hydrogen sulfide in living cells. ChemistrySelect, 2016, 1(11): 2581–2585
125. Kaushik R, Ghosh A, Singh A, Jose D A. Colorimetric sensor for the detection of H_2S and its application in molecular half-subtractor. Analytica Chimica Acta, 2018, 1040: 177–186
126. Wang C, Cheng X, Tan J, Ding Z, Wang W, Yuan D, Li G, Zhang H, Zhang X. Reductive cleavage of C = C bonds as a new strategy for turn-on dual fluorescence in effective sensing of H_2S. Chemical Science (Cambridge), 2018, 9(44): 8369–8374
127. Choi M G, Cha S, Lee H, Jeon H L, Chang S K. Sulfide-selective chemosignaling by a Cu^{2+} complex of dipicolylamine appended fluorescein. Chemical Communications, 2009, (47): 7390–7392
128. Hou J T, Liu B Y, Li K, Yu K K, Wu M B, Yu X Q. Two birds with one stone: multifunctional and highly selective fluorescent probe for distinguishing Zn^{2+} from Cd^{2+} and selective recognition of sulfide anion. Talanta, 2013, 116: 434–440
129. Yue X, Zhu Z, Zhang M, Ye Z. Reaction-based turn-on electrochemiluminescent sensor with a ruthenium(II) complex for selective detection of extracellular hydrogen sulfide in rat brain. Analytical Chemistry, 2015, 87(3): 1839–1845
130. Lv H J, Ma R F, Zhang X T, Li M H, Wang Y T, Wang S, Xing G W. Surfactant-modulated discriminative sensing of HNO and H_2S with a Cu^{2+}-complex-based fluorescent probe. Tetrahedron, 2016, 72(35): 5495–5501
131. Sasakura K, Hanaoka K, Shibuya N, Mikami Y, Kimura Y, Komatsu T, Ueno T, Terai T, Kimura H, Nagano T. Development of a highly selective fluorescence probe for hydrogen sulfide. Journal of the American Chemical Society, 2011, 133(45): 18003–18005
132. Wu H, Krishnakumar S, Yu J, Liang D, Qi H, Lee Z W, Deng L W, Huang D. Highly selective and sensitive near-infrared-fluorescent probes for the detection of cellular hydrogen sulfide and the imaging of H_2S in mice. Chemistry, an Asian Journal, 2014, 9(12): 3604–3611
133. Ye Z, An X, Song B, Zhang W, Dai Z, Yuan J. A novel dinuclear ruthenium(II)-copper(II) complex-based luminescent probe for hydrogen sulfide. Dalton Transactions (Cambridge, England), 2014, 43(34): 13055–13060
134. Palanisamy S, Lee L Y, Wang Y L, Chen Y J, Chen C Y, Wang Y M. A water soluble and fast response fluorescent turn-on copper complex probe for H_2S detection in zebra fish. Talanta, 2016, 147: 445–452
135. Cao X, Lin W, He L. A near-infrared fluorescence turn-on sensor for sulfide anions. Organic Letters, 2011, 13(17): 4716–4719
136. Hou F, Huang L, Xi P, Cheng J, Zhao X, Xie G, Shi Y, Cheng F, Yao X, Bai D, Zeng Z. A retrievable and highly selective fluorescent probe for monitoring sulfide and imaging in living cells. Inorganic Chemistry, 2012, 51(4): 2454–2460
137. Hou F, Cheng J, Xi P, Chen F, Huang L, Xie G, Shi Y, Liu H, Bai D, Zeng Z. Recognition of copper and hydrogen sulfide *in vitro* using a fluorescein derivative indicator. Dalton Transactions (Cambridge, England), 2012, 41(19): 5799–5804
138. Kar C, Adhikari M D, Ramesh A, Das G. NIR- and FRET-based sensing of Cu^{2+} and S^{2-} in physiological conditions and in live cells. Inorganic Chemistry, 2013, 52(2): 743–752
139. Tang L, Dai X, Cai M, Zhao J, Zhou P, Huang Z. Relay recognition of Cu^{2+} and S^{2-} in water by a simple 2-(2′-aminophenyl) benzimidazole derivatized fluorescent sensor through modulating ESIPT. Spectrochimica Acta. Part A: Molecular and Biomolecular Spectroscopy, 2014, 122: 656–660
140. Qian Y, Lin J, Liu T, Zhu H. Living cells imaging for copper and hydrogen sulfide by a selective “on-off-on” fluorescent probe. Talanta, 2015, 132: 727–732

141. Meng Q, Shi Y, Wang C, Jia H, Gao X, Zhang R, Wang Y, Zhang Z. NBD-based fluorescent chemosensor for the selective quantification of copper and sulfide in an aqueous solution and living cells. Organic & Biomolecular Chemistry, 2015, 13(10): 2918–2926
142. Hai Z, Bao Y, Miao Q, Yi X, Liang G. Pyridine-biquinoline-metal complexes for sensing pyrophosphate and hydrogen sulfide in aqueous buffer and in cells. Analytical Chemistry, 2015, 87(5): 2678–2684
143. Liu J, Guo X, Hu R, Liu X, Wang S, Li S, Li Y, Yang G. Molecular engineering of aqueous soluble triarylboron-compound-based two-photon fluorescent probe for mitochondria H_2S with analyte-anduced finite aggregation and excellent membrane permeability. Analytical Chemistry, 2016, 88(1): 1052–1057
144. Yang L, Wang J, Yang L, Zhang C, Zhang R, Zhang Z, Liu B, Jiang C. Fluorescent paper sensor fabricated by carbazole-based probes for dual visual detection of Cu^{2+} and gaseous H_2S. RSC Advances, 2016, 6(61): 56384–56391
145. Wang P, Wu J, Di C, Zhou R, Zhang H, Su P, Xu C, Zhou P, Ge Y, Liu D, Liu W, Tang Y. A novel peptide-based fluorescence chemosensor for selective imaging of hydrogen sulfide both in living cells and zebrafish. Biosensors & Bioelectronics, 2017, 92: 602–609
146. Rajasekaran D, Venkatachalam K, Periasamy V. "On-off-on" pyrene-based fluorescent chemosensor for the selective recognition of Cu^{2+} and S^{2-} ions and its utilization in live cell imaging. Applied Organometallic Chemistry, 2020, 34(3): e5342
147. Qu X, Li C, Chen H, Mack J, Guo Z, Shen Z. A red fluorescent turn-on probe for hydrogen sulfide and its application in living cells. Chemical Communications, 2013, 49(68): 7510–7512
148. Sun M, Yu H, Li H, Xu H, Huang D, Wang S. Fluorescence signaling of hydrogen sulfide in broad pH range using a copper complex based on BINOL-benzimidazole ligands. Inorganic Chemistry, 2015, 54(8): 3766–3772
149. Li X, Yang C, Wu K, Hu Y, Han Y, Liang S H. A highly specific probe for sensing hydrogen sulfide in live cells based on copper-initiated fluorogen with aggregation-induced emission characteristics. Theranostics, 2014, 4(12): 1233–1238
150. Kawagoe R, Takashima I, Usui K, Kanegae A, Ozawa Y, Ojida A. Rational design of a ratiometric fluorescent probe based on arene-metal-ion contact for endogenous hydrogen sulfide detection in living cells. ChemBioChem, 2015, 16(11): 1608–1615
151. Ma F, Sun M, Zhang K, Yu H, Wang Z, Wang S. A turn-on fluorescent probe for selective and sensitive detection of hydrogen sulfide. Analytica Chimica Acta, 2015, 879: 104–110
152. Gupta N, Reja S I, Bhalla V, Kumar M. Fluorescent probes for hydrogen polysulfides (H_2S_n, $n > 1$): from design rationale to applications. Organic & Biomolecular Chemistry, 2017, 15(32): 6692–6701
153. Liu C, Chen W, Shi W, Peng B, Zhao Y, Ma H, Xian M. Rational design and bioimaging applications of highly selective fluorescence probes for hydrogen polysulfides. Journal of the American Chemical Society, 2014, 136(20): 7257–7260
154. Ma J, Fan J, Li H, Yao Q, Xu F, Wang J, Peng X. A NIR fluorescent chemodosimeter for imaging endogenous hydrogen polysulfides via the CSE enzymatic pathway. Journal of Materials Chemistry. B, Materials for Biology and Medicine, 2017, 5(14): 2574–2579
155. Li K B, Chen F Z, Yin Q H, Zhang S, Shi W, Han D M. A colorimetric and near-infrared fluorescent probe for hydrogen polysulfides and its application in living cells. Sensors and Actuators. B, Chemical, 2018, 254: 222–226
156. Zhao L, Sun Q, Sun C, Zhang C, Duan W, Gong S, Liu Z. An isophorone-based far-red emitting ratiometric fluorescent probe for selective sensing and imaging of polysulfides. Journal of Materials Chemistry. B, Materials for Biology and Medicine, 2018, 6(43): 7015–7020
157. Hou P, Wang J, Fu S, Liu L, Chen S. A new turn-on fluorescent probe with ultra-large fluorescence enhancement for detection of hydrogen polysulfides based on dual quenching strategy. Spectrochimica Acta. Part A: Molecular and Biomolecular Spectroscopy, 2019, 213: 342–346
158. Li W, Zhou S, Zhang L, Yang Z, Chen H, Chen W, Qin J, Shen X, Zhao S. A red emitting fluorescent probe for sensitively monitoring hydrogen polysulfides in living cells and zebrafish. Sensors and Actuators. B, Chemical, 2019, 284: 30–35
159. Liu J, Yin Z. A resorufin-based fluorescent probe for imaging polysulfides in living cells. Analyst (London), 2019, 144(10): 3221–3225
160. Zhang C, Sun Q, Zhao L, Gong S, Liu Z. A BODIPY-based ratiometric probe for sensing and imaging hydrogen polysulfides in living cells. Spectrochimica Acta. Part A: Molecular and Biomolecular Spectroscopy, 2019, 223: 117295
161. Fang Q, Yue X, Han S, Wang B, Song X. A rapid and sensitive fluorescent probe for detecting hydrogen polysulfides in living cells and zebra fish. Spectrochimica Acta. Part A: Molecular and Biomolecular Spectroscopy, 2020, 224: 117410
162. Wang C, Xu J, Ma Q, Bai Y, Tian M, Sun J, Zhang Z. A highly selective fluorescent probe for hydrogen polysulfides in living cells based on a naphthalene derivative. Spectrochimica Acta. Part A: Molecular and Biomolecular Spectroscopy, 2020, 227: 117579
163. Zhao X, He F, Dai Y, Ma F, Qi Z. A single fluorescent probe for one- and two-photon imaging hydrogen sulfide and hydrogen polysulfides with different fluorescence signals. Dyes and Pigments, 2020, 172: 107818
164. Ren Y, Zhang L, Zhou Z, Luo Y, Wang S, Yuan S, Gu Y, Xu Y, Zha X. A new lysosome-targetable fluorescent probe with a large Stokes shift for detection of endogenous hydrogen polysulfides in living cells. Analytica Chimica Acta, 2019, 1056: 117–124
165. Han Q, Liu X, Wang X, Yin R, Jiang H, Ru J, Liu W. Rational design of a lysosomal-targeted ratiometric two-photon fluorescent probe for imaging hydrogen polysulfides in live cells. Dyes and Pigments, 2020, 173: 107877
166. Zhang X, Zhang L, Gao M, Wang Y, Chen L. A near-infrared fluorescent probe for observing thionitrous acid-mediated hydrogen polysulfides formation and fluctuation in cells and *in vivo* under hypoxia stress. Journal of Hazardous Materials, 2020, 396: 122673
167. Fang Y, Chen W, Shi W, Li H, Xian M, Ma H. A near-infrared fluorescence off-on probe for sensitive imaging of hydrogen polysulfides in living cells and mice *in vivo*. Chemical Commu-

nications, 2017, 53(62): 8759–8762

168. Yang F, Gao H, Li S S, An R B, Sun X Y, Kang B, Xu J J, Chen H Y. A fluorescent tau-probe: quantitative imaging of ultra-trace endogenous hydrogen polysulfide in cells and *in vivo*. Chemical Science (Cambridge), 2018, 9(25): 5556–5563
169. Hoskere A A, Sreedharan S, Ali F, Smythe C G, Thomas J A, Das A. Polysulfide-triggered fluorescent indicator suitable for super-resolution microscopy and application in imaging. Chemical Communications, 2018, 54(30): 3735–3738
170. Choi H J, Lim C S, Cho M K, Kang J S, Park S J, Park S M, Kim H M. A two-photon ratiometric probe for hydrogen polysulfide (H_2S_n): increase in mitochondrial H_2S_n production in a Parkinson's disease model. Sensors and Actuators. B, Chemical, 2019, 283: 810–819
171. Liang L, Li W, Zheng J, Li R, Chen H, Yuan Z. A new lysosome-targetable fluorescent probe for detection of endogenous hydrogen polysulfides in living cells and inflamed mouse model. Biomaterials Science, 2020, 8(1): 224–231